GEOLOGICAL SURVEY OF CANADA
OPEN FILE 7056

Organic Petrology and vitrinite thermal maturation profiles for eight Yukon petroleum exploration wells in Eagle Plain and Liard basins

J. Reyes, S. Saad, and L.S. Lane

2013

Natural Resources Canada | Ressources naturelles Canada

Canada

GEOLOGICAL SURVEY OF CANADA
OPEN FILE 7056

Organic Petrology and vitrinite thermal maturation profiles for eight Yukon petroleum exploration wells in Eagle Plain and Liard basins

J. Reyes, S. Saad, and L.S. Lane

2013

doi:10.4095/293110

This publication is available for free download through GEOSCAN (http://geoscan.ess.nrcan.gc.ca/).

Recommended citation
Reyes, J., Saad, S., and Lane, L.S., 2013. Organic Petrology and vitrinite thermal maturation profiles for eight Yukon petroleum exploration wells in Eagle Plain and Liard basins; Geological Survey of Canada, Open File 7056, 56 p. doi:10.4095/293110

Table of Contents

Abstract

Eight Yukon petroleum exploration wells were sampled for organic petrology and vitrinite reflectance thermal maturity. Seven wells are located in Eagle Plain, northern Yukon, and one is from Liard Plateau in southeastern Yukon. Where possible, the stratigraphic tops used in the interpretations reflect the currently available biostratigraphy. Kerogen type is dominated by marine to marginal marine, Type II and Type II/III; and pyrite is commonly found in association with the kerogen.

Over much of Eagle Plain basin, Late Devonian to Albian strata are within the oil window. Higher reflectance values, into the dry gas zone at depth, are recorded toward the basin margins where older rocks are exposed. Absence of a maturity discontinuity at the sub-Mesozoic unconformity indicates that the thermal maximum post-dates Albian and predates early Tertiary exhumation.

In the Beaver YT G-01 well in Liard Basin, the Late Devonian succession lies within the wet gas to dry gas windows whereas the Carboniferous section is within the oil generation window.

Introduction

As part of the basin analysis component of the GEM Yukon Basins Project, a suite of petroleum exploration wells across Yukon were sampled for biostratigraphy, organic geochemistry and organic petrology. In general, the purposes include improved stratigraphic correlation among wells, improved characterization and correlation of organic matter types and improved documentation of the thermal evolution of Yukon's basins. This report presents organic petrology data for eight Yukon petroleum exploration wells, seven from Eagle Plain, northern Yukon and one from Liard Plateau, southeastern Yukon.

In four of the eight wells summarized here, (S. Tuttle N-05, N. Hope N-53, Blackstone D-77 and Shaeffer Creek O-22), the bulk of the data are reproduced from Link (1988; see Link and Bustin, 1989). The rest of the data in these wells and all of the data in the other four wells (Parkin D-61, Ellen C-24, Birch B-34, Beaver G-01) consist of entirely new analyses for the GEM Yukon Basins project. For all of these wells core and cuttings were sampled for geochemical, petrological and paleontological analyses, including 114 samples which were run for vitrinite reflectance (%Ro). The primary purpose in analysing additional samples from the previously studied wells was to provide a robust calibration between the important earlier thermal history work of Link and Bustin (1989) and

the new data presented through the current project. Analytical procedures based on optical microscopy are particularly sensitive to variations from one laboratory to another, due to differing methodologies, equipment, operators and technology. This is particularly so when the analyses being compared were done twenty years apart. By ensuring some overlap between the 1989 and current work, some level of integrated interpretation is possible between the two separate datasets in order to determine basin wide thermal maturity trends.

The new quantitative vitrinite reflectance data are supplemented by a short summary of the qualitative analysis of the dispersed organic matter (DOM)/kerogen assemblages and microlithotypes, including morphological and fluorescence properties of vitrinite, liptinite macerals and solid bitumen, hydrocarbon fluid inclusions and the presence of microfossils. Such information provides an additional means for determining the thermal and paleodepositional history of each stratigraphic formation and for assessing the overall source rock potential of the basin for hydrocarbon and gas exploration.

Geological Setting

Seven of the wells included in this report are located in Eagle Plain, northern Yukon, a weakly deformed intermontane basin bordered on all sides by ranges uplifted during latest Cretaceous and Paleogene orogenesis in the northern Canadian Cordillera (e.g., Lane and Dietrich, 1995; Lane, 1998). Its foundation comprises part of the Yukon stable block, an early Paleozoic carbonate platform at the northwest margin of Laurentia, partially separated from the cratonic interior platform by the coeval Richardson Trough (Morrow, 1999).

Late Devonian and Early Carboniferous Ellesmerian deformation, encroaching from the north, buried much of the area under a thick succession of orogenic foredeep deposits and generated east-west trending folds and thrust faults on its northern margin (Lane, 2007). Late Paleozoic deep marine basinal clastic and carbonate deposits are preserved in the southern part of the basin, but they have been removed from the northern part by Permian and younger erosion (e.g., Richards et al., 1997; Dixon, 1998).

Although Jurassic and Early Cretaceous rocks are locally preserved around its margins, across much of the basin Albian strata lie directly on rocks of Late Devonian to Permian age. Initially, marine shelf clastic rocks of the Whitestone River Formation were deposited across the basin, followed by the

Albian and younger Eagle Plain Group, interpreted as clastic foredeep deposits derived from the Ogilvie and Wernecke ranges to the south, began to spread northward and westward across the basin (Dixon, 1992; Jackson et al., 2011; Haggart et al., 2013).

Proven oil and gas reserves are known in the Chance and Birch fields in southern Eagle Plain, where the reservoirs are in Carboniferous clastic rocks (e.g., Osadetz et al., 2005).

The Beaver YT G-01 gas well is located in the Liard Plateau of southeastern Yukon, near the boundary with British Columbia. It was drilled on the Mount Martin anticline, one of the large en echelon structures dominating the southern end of the Franklin range in the foreland of the northern Canadian Cordillera (Fallas, 2006). This area, marginal to the extensive Liard Basin, is underlain by strata transitional from platformal carbonates typical of the Western Canada Sedimentary Basin and fine clastics of Selwyn Basin. Although the existing gas field taps Manetoe facies dolomite in the Nahanni Formation, late Paleozoic strata are prospective for shale gas.

Well Locations& Hydrocarbon Systems

Eagle Plain Basin is one of eight prospective basins in the Yukon identified as having significant oil and gas potential. To date, 34 wells have been drilled in the basin, many of which show evidence of the presence of conventional oil and gas. Figure 1 shows the locations of the seven wells in Eagle Plain Basin discussed in this study.

The stratigraphic nomenclature for Eagle Plain Basin used in this report is modified from Pigage (2009) and Jackson (2012) Figure 2. Paleozoic strata are dominated by limestones and shales with intervening sandstone units of late Devonian to Permian age. Cretaceous strata are dominated by alternating sandstone and shale deposits. A major unconformity exists below the Albian Whitestone River Formation where late Permian to Early Cretaceous strata are missing. Potential source rocks in the basin include the Road River Group and the Canol, Ford Lake, Hart River and Blackie formations. Oil and gas discoveries were made in the Chance Sandstone Member of the Hart River Formation. Other potential reservoir rocks based on gas shows include the Ogilvie, Imperial, Tuttle and Jungle Creek formations (Morrow et al., 2006).

Liard Plateau is part of the gas-producing Liard Basin that lies within southeast Yukon, southwest Northwest Territories and northeast British Columbia. A total of 13 wells have been drilled in the

Yukon part of this basin and have shown significant gas potential. Beaver G-01 is the only well in this study that is located in Liard Basin (Figure 3).

A stratigraphic section for Liard Basin is shown in Figure 4 (modified from Jones and Gal, 2007). In this basin, the Paleozoic strata also tend to be dominated by carbonates (Kotcho, Muskwa, Nahanni formations) and shales (Besa River and Fort Simpson formations, Horn River Group) as well as the Mattson Formation sandstone and Fantasque Formation chert. Mesozoic strata are composed of shales with subsidiary sandstones (e.g. Chinkeh and Scatter formations). No depositional record exists for the Jurassic period throughout this basin. Proven source rocks include the Horn River Group and Besa River Formation, whereas the Garbutt and Toad formations are probable source rocks. Gas discoveries have been made within the Nahanni, Horn River, Mattson and Chinkeh formations. Other possible reservoir rocks include the Besa River, Kotcho, and Fantasque formations (Morrow et al., 2006).

Vitrinite Reflectance

Vitrinite reflectance has been used widely to calibrate thermal history and time-temperature models for stratigraphic successions within sedimentary basins, particularly for evaluating oil and gas generation (Powell and Snowdon, 1983; Tyson, 1987; Stasiuk, 1991; Potter et al., 1993a and 1993b; Potter, 1998; Stasiuk and Fowler, 2004). Since the rate of coalification reactions and percent reflectance in oil (%Ro) of huminite, vitrinite and bitumen increase with increasing temperature (Jacob, 1989), these macerals provide an indirect geothermometer for evaluating the thermal conditions during sediment burial. The oil and gas generation potential of sedimentary rocks in general is determined by factors including geology, total organic carbon, organic type (facies), paleodepositional environment and burial history (Tissot & Welte, 1984; Huc, 1988, 1990; Cameron et al., 1994; Cole et al., 1994; Potter, 1998; Stasiuk and Fowler, 2004). Source rocks deposited in dysaerobic to anoxic, marine depositional environments with moderate to high organic productivity such as the continental shelf and upper slopes (Figure 5) are the most hydrocarbon prone regions (Demaison & Moore, 1980; Tyson, 1987; Cole et al, 1994; Potter, 1998; Stasiuk and Fowler, 2004). The amount and type of oil (e.g. crude oil) and/or gas (e.g. condensate, wet gas, dry gas) produced by a sedimentary source rock depends upon the organic facies or kerogen type (Figure 6) in the source rock and its diagenetic condition (Tissot et al., 1974; Leythaeuser et al., 1980, Potter, 1998).

Methodology

Vitrinite Reflectance Methods

Standard procedures for organic petrology based on Mackowsky (1982) are generally followed. Unwashed cuttings and core samples were prepared in a similar way by crushing them into 1-5 mm particulates, with many also sized to ~ 1 cm cubes. The samples were then mounted in a one inch mould using epoxy and were then polished using four types of polishing materials. Random reflectance ($\%Ro_{random}$) measurements were carried out using a Leitz reflected light microscope with a 50X oil immersion objective and white (halogen; 546nm) and fluorescent (HBO 100W) light sources. The actual %Ro measurements were taken by the Leitz MPV II – COMBI photometer system attached to a pc-controller system for %Ro data collection which was mounted on top of the microscope. Reflectance was calibrated using Schott precision glass standards with 0.506, 1.025, and 1.817 %Ro refractive index. The microscope was calibrated before and mid-way through each analysis in accordance with standard procedures stated in Mackowsky (1982); International Committee for Coal Petrology (1975, 1994) and Bustin et al. (1983). The oil used was halogen free/low fluorescence with a refractive index of $n_e = 1.518$ at 23^oC. Reflectance measurements were made on vitrinite (huminite, eu-ulminite B and telovitrinite A are the preferred macerals for measurement wherever possible), bituminite and bitumen macerals, together with alginite and sporinite-derived macerals. In the absence of vitrinite, vitrinite equivalent ($\%Ro_{equivalent}$) was calculated using the measured reflectance of primary bitumen ($\%Ro_{Bitumen}$) or in some cases pyrobitumen ($\%Ro_{Pyrobitumen}$) and the Jacob (1989) equation (where applicable).

Thermal Maturity and Qualitative Analysis of Dispersed Organic Matter (DOM)

The results of the quantitative analysis of thermal maturity using vitrinite reflectance are presented in plots showing the sample depth, stratigraphic location and corresponding lithology (Figures 7, 8, 10-13,16 and 18). Tables 1 through 8 list the formation, depth, organic matter (OM) type, average %Ro, standard deviation (SD), the number of particles (N) measured for each sample and sample type for all eight wells. The reworked vitrinite particles were measured qualitatively to determine the thermal maturity and origin of the macerals. The measured %Ro was plotted against the known thermal maturity parameters for determining type of oil and gas expected at each level of maturity. Observations of the organic maceral assemblage and kerogen type, by source, for the formations in each well are discussed below. They provide some evidence to overall paleodepositional environment

of the sampled strata. The organic matter assemblages observed in most of the wells are consistent with Type II (by source, presence of alginite and sporinite) deposited in deep marine to shallow, barred to possibly deltaic paleodepositional environments. The quantity, size and morphology of the terrestrial plant derived macerals (spores, coaly lenses, inertinite, etc.) found in the matrix also suggest the relative water level and distance from its source. All this information combined can be used to determine the type of hydrocarbon that can be generated by applying the hydrocarbon generation model (Figure 6) (Stasiuk 1991) in conjunction with the measured thermal maturity.

Ellen C-24 well

The thermal maturity of all the core samples (Figure 7) has reached the oil generating window with the majority of values corresponding to the peak oil expulsion window. The shallowest sample, taken from the Lower Cretaceous Parkin Formation, has a thermal maturity of 0.65 %Ro. Near the depth of the sub-Mesozoic unconformity, located at approximately 1300 m, thermal maturity (0.73 to 0.99 %Ro) has reached the oil expulsion window. This maturity level continues downward through most of the Imperial/Tuttle succession down to the last sample analyzed (2173 m) from this well (Table 1).

Parkin and Whitestone River formations (334/09, 335/09)

The Parkin Formation (334/09) organic matter assemblage consists of Type II alginite-rich, brown carbonate shale with mostly yellow-fluorescing prasinophyte alginite and rare amounts of reworked vitrinite lenses. The Whitestone River Formation (335/09) has similar lithology and organic matter assemblages with the additional inclusion of *Tasmanites* sp. alginite, siliceous microfossils and sporinite macerals.

Imperial/Tuttle Formation (336/09 to 351/09)

The Imperial/Tuttle succession is the most sampled interval in the Ellen C-24 well. The top of the succession (336/09, 337/09, 338/09, 339/09, 340/09; Table 1) consists of brown, carbonate shale with minor amounts of pyrite minerals and yellow fluorescing alginite (mainly prasinophyte and rare amount of *Tasmanites* sp.). Trace amounts of siliceous microfossils, yellow fluorescing sporinite macerals showing zonation and reworked vitrinite lenses are also observed.

Slightly lower in the Imperial/Tuttle succession, the samples (341/09, 342/09) show a carbonate shale, very fine grain sandstone matrix with minor amounts of alginite-derived stylocumulates, organic

matter and some yellow to orange fluorescing liptodetrinite inclusions mainly brecciated between intergranular pores. It is possible that dolomitizing fluid carrying solid bitumen and oil, possibly from older source rocks, penetrated microfractures and pores of the carbonate shale matrix as suggested by higher thermal maturity values compared to the in-situ host rocks. Major amounts of hydrocarbon fluid inclusions associated with calcite, dolomite and quartz grains mainly within tight intergranular pores and microfractures are also observed in some of the matrix.

Lower in the succession (below ~1667 m) the samples (343/09 to 351/09) consist of carbonate shale matrix with major amounts of long lenses of alginite-derived kerogen and framboidal pyrite, some yellow to orange fluorescing alginite (prasinophyte, *Tasmanites* sp. and *Leiosphaeridia* sp.) and solid bitumen inclusions mostly within black shaly matrix. The carbonate matrix tends to be organically leaner than the black shale matrix microlaminates. There is a minor presence of red fluorescing granular solid bitumen brecciated between intergranular pores of the rare siltstone matrix. Rare amount of orange fluorescing sporinite macerals showing zonation, alginite-derived stylocumulates and reworked vitrinite lenses are also found in the matrix. Hydrocarbon fluid inclusions are observed in some small quartz and calcite grains. The overall maceral assemblage of the Imperial and Tuttle formations is marine Type II kerogen by source.

N Hope N-53 well

The data from this well (Figure 8; Table 2) include five new analyses (all cuttings) and 40 older Link (1988) data. The new data fall within the scatter of the older data. The Lower Cretaceous strata located near the surface are marginally mature but attain oil window maturity levels near 250 m depth. All of the data from Link fall within the oil window and 18 samples fall within the peak oil generation stage. These 18 samples were taken from the Whitestone River Formation and Imperial/Tuttle succession (Table 2). Four out of five samples from the GSC plot within the oil window and one sample from the Whitestone River Formation plots within the peak oil generation stage. Though the coefficient of determination (R^2) for the GSC data (0.96) is much higher than that of the Link data (0.74), the GSC has limited data points thereby reducing the level of confidence as compared to Link's 1988 data.

Whitestone River Formation (189/09 – 190/09)

The Albian sediments of the Whitestone River Formation (189/09) are composed of alginite-rich carbonate shale. The alginite is mostly in the form of small, unicellular, yellow-fluorescing

prasinophyte with very rare non-fluorescing sporinite macerals. Rare reworked vitrinite and inertinite macerals are also observed. Deeper in the Whitestone River Formation (190/09) the samples show carbonate-shale with some reworked sandstone containing minor amounts of reworked vitrinite and bitumen lenses (Type II kerogen by source). Also observed are rare fluorescing unicellular alginite macerals mainly associated with the younger caved carbonate-shale matrix and very rare hydrocarbon fluid inclusions within quartz and calcite mineral matrices.

Imperial/Tuttle Succession (191/09 – 193/09)

Throughout the Imperial/Tuttle succession, samples 191/09, 192/09, and 193/09 have similar organic matter assemblages to the deeper samples of the Whitestone River Formation (190/09). The deepest sample (193/09) also shows evidence of a highly reworked matrix with minor organic matter content, mostly in the form of bitumen macerals (associated mainly with the sandstone matrix) and amorphinite (associated with the carbonate-shale matrix). Figure 9 shows three photomicrographs displaying bitumen macerals and pyrite (Type II kerogen by source).

Shaeffer Creek O-22 well

The data from this well (Figure 10; Table 3) are from cuttings samples including nine new analyses and 48 previous analyses from Link (1988). The new analyses are similar to those of Link (1988) below approximately 1000 m depth. Although the new analyses show slightly higher maturity at all depths, the new and older data converge near 2500 m. Only above 1000 m does the new trend clearly diverge from the older one, with the Cretaceous section significantly more mature than previously recorded, although still immature. Both data sets have a similar coefficient of determination (R^2) value near 0.90, indicating that the regression line for each set fits the data quite well.

The data from Link (1988) show that 24 samples are within marginally mature to mature (0.5 to 1.3% Ro) range of thermal maturity, seven of which attained the peak oil generation stage (0.7 to 1.0%). These seven samples are found within Devonian strata of the Imperial/Tuttle/Ford Lake, Canol and Ogilvie formations. The GSC data show that nine samples reached oil window conditions, three of which attained the peak oil generation stage. These three lie within the Upper Devonian-Carboniferous strata of the Imperial/Tuttle/Ford Lake formations.

Parkin Formation (67/09)

Only one sample (67/09) is taken from the Early Cretaceous Parkin Formation at 305 m depth. The dispersed organic matter found in the sample includes small vitrinite to large coaly matrix brecciated within the shaly siltstone with average reflectance of 0.54 %Ro. The coal macerals contain yellow fluorescing sporinite and pollen grain, resinite, fluoramorphinite and bituminite maceral inclusions (Type II/III kerogen by source). Bright fluorescing thin walled unicellular alginite, possibly prasinophyte is also observed. Allochthonous inertinite and vitrinite macerals are also noted in this sample.

Whitestone River Formation (68/09)

Sample 68/09 matrix consists of highly reworked pyrite-rich shaly siltstone with a high amount of inertinite macerals. Other organic matter observed include liptinite maceral includes yellow to orange fluorescing sporinite, pollen, bitumen and fluoramorphinite with bright fluorescing unicellular alginite (possibly prasinophyte) inclusions. Orange fluorescing bituminite macerals with 0.26 %Ro are also observed in the matrix. Some matrix shows evidence of possible contact with dolomitizing fluid as indicated by some brecciated high reflecting vitrinite maceral inclusions. The thermal maturities of these samples indicate that they reached the early stage of oil generation.

Imperial/Tuttle/Ford Lake formations (69/09 to 74/09, 77/09)

Samples from Imperial, Tuttle and Ford Lake Formations are defined by pyrite-rich (framboidal) shaly siltstone of highly reworked sandstone and shaly carbonate matrices. The siltstone matrix also contains rare amount of yellow to orange fluorescing sporinite, trace amount of yellow fluorescing prasinophyte alginite and bituminite macerals. Sandstone and carbonate matrices contain minor amounts of yellow to orange fluorescing sporinite, bitumen, and rare fluoramorphinite with bright fluorescing unicellular prasinophyte alginite inclusions. Rare dolomite matrix with rare kerogen inclusions are also observed in this sample. Yellow fluorescing hydrocarbon fluid inclusions are observed between micropores and trapped within carbonate fractures. Several reworked petrified wood matrices showing botanical structure are observed in the upper part of the formation, possibly caved? The complexity of the DOM macerals assemblages suggests a Type II/III kerogen type. Some siltstone particles with high reflecting bitumen maceral suggest possible contact with epigenetic dolomitizing fluid. Trace amount of yellow fluorescing hydrocarbon inclusions are also found within fractures of quartz and dolomite mineral.

Birch B-34 well

The data for the Birch B-34 well (Figure 11; Table 4) comes from 14 core and 12 cuttings samples analyzed under the GEM project Most of the data points are below the Permian unconformity at about 290 m. Near 300 m depth the thermal maturity is approaching oil window reflectance levels. The maturity level approaches the gas condensate window near 1500 m depth. All of the samples either reached early maturity (Whitestone River Formation) or peak oil generation window(Jungle Creek to Hart River formations).

Whitestone River Formation (246/13 and 133/10)

Two samples are taken from Whitestone River Formation near the Whitestone River-Jungle Creek unconformity. Both samples consist of carbonate-shale matrix. The dispersed organic matters observed are yellow fluorescing sporinite (some showing ornamentation) and trace amounts of yellow fluorescing prasinophyte and dinoflagellate alginite. The measured thermal maturity is 0.61 and 0.64 %Ro, respectively, just below the peak oil generation window. There are trace amounts of orange to brown fluorescing bitumen macerals and yellow-fluorescing soluble organics. Minor amounts of framboidal pyrite inclusion within the spent kerogen and terrestrial plant-derived inertinite macerals are also observed in the matrix (Type II kerogen by source).

Jungle Creek Formation (134/10 to 136/10, 247/13 to 248/13)

The upper Jungle Creek Formation is an organically-lean, reworked shaly siltstone matrix with trace amounts of orange fluorescing sporinite macerals brecciated between carbonate grains and greenish-yellow fluorescing hydrocarbon fluid inclusions trapped within carbonate grain microfractures. Trace amounts of brown-fluorescing bitumen macerals are also observed. The last sample (248/13) is mainly shaly very fine grain sandstone to siltstone matrix showing minor amount of orange fluorescing sporinite and inertinite maceral. Soluble organics staining between intergranular pores is also observed in this sample. The thermal maturity of the samples (0.67 to 0.75 %Ro, respectively, Table 4) suggests they reached peak oil generation, which correlates with observed fluorescence properties of the hydrocarbon fluid inclusions and sporinite macerals (Type II/III kerogen by source).

Ettrain Formation (249/13)

A single sample is analysed from this formation, it mainly consists of silty shale and siltstone matrix. There are minor amounts of mostly dull yellow to reddish-orange fluorescing sporinite and cutinite

maceral with trace amounts of yellow fluorescing small unicellular alginite, possibly prasinophyte. The majority of the observed dispersed organic matter is reworked coaly vitrinite and inertinite macerals.

Blackie Formation (137/10 to 142/10, 250/13 to 252/13)

Samples from the upper portion of the Blackie Formation (137/10, 138/10) consist of carbonate-shale with minor amounts of framboidal pyrite and liptinite macerals. Minor amounts of yellow fluorescing alginite (prasinophyte and possibly filamentous alginite) and trace amounts of yellow to orange fluorescing sporinite macerals showing some ornamentation are present. There are trace amounts of orange to brown fluorescing bitumen macerals and yellow fluorescing soluble organics. Trace amounts of terrestrial plant-derived inertinite macerals are also observed in the matrix. Some vitrinite reflectance measurements in these samples are suppressed due to the presence of soluble organics in some matrices. Slightly lower in the formation (139/10, 140/10) the lithology transitions to an organically-lean carbonate shale with trace amounts of orange to non-fluorescing cutinite, liptinite and sporinite (some showing ornamentation), framboidal pyrite and yellow-fluorescing alginite macerals (prasinophyte and possibly filamentous alginite). Trace amount of orange to brown fluorescing solid bitumen macerals and terrestrial plant-derived inertinite and vitrinite macerals are also observed in the matrix. The five samples (141/10, 142/10, 250/13 to 252/13) taken from the lower section of the Blackie formation have a thermal maturity range between 0.79 to 0.89 %Ro. They are mostly an organically-lean matrix with trace amounts of organic-rich carbonate-shale microlaminate. The DOM consists of orange to non-fluorescing sporinite and cutinite macerals, yellow fluorescing alginite (prasinophyte), reddish-orange to non-fluorescing bitumen macerals and fluoramorphinite. Orange to brown fluorescing matrix bituminite, hebamorphinite and framboidal pyrite are also observed in the organic-rich matrices. Trace amounts of terrestrial plant-derived inertinite and vitrinite macerals are also observed in the matrix. Higher reflecting allochthonous vitrinite and inertinite macerals are also noted (Type II/III kerogen by source).

Hart River Formation (143/10 to 146/10, 253/13 to 257/13)

There are a total of nine samples from this formation consisting of four core and five cutting samples. They are represented by organic-rich black carbonate-shale to framboidal pyrite-rich siltstone matrix, organically lean very fine grain sandstone/siltstone, and organically lean calcareous limestone, and organic and framboidal pyrite rich dark brown silty shale. The` thermal maturity of these sampled strata ranges from 1.00 to 1.19 %Ro which equates to the latter stage of the oil window. The

organically-rich, black carbonate-shale has an organic maceral assemblage consisting of interconnected networks of amorphous kerogen derived mostly from marine alginite and trace sporinite macerals (Type II kerogen by source). There are minor amounts of orange to brown fluorescing alginite and sporinite macerals and major amounts of solid bitumen between microfractures and pore spaces, some of which show weak reddish fluorescence properties. Rare yellow fluorescing hydrocarbon fluid inclusions are also observed trapped within quartz grain microfractures and intracrystalline growth zones. Solid isotropic migrabitumen is associated with saddle dolomite, limestone pores and microfractures in sample 143/10. Primary isotropic bitumen and secondary isotropic migrabitumen are also observed in sample 144/10. Sample 144/10 shows suppressed secondary isotropic bitumen. Slightly deeper in the Hart River Formation (145/10) the sample is an organically-lean sandstone matrix with mostly framboidal pyrite-rich amorphous stylocumulates, granular amorphinite and trace amounts of isotropic solid bitumen macerals. Trace amounts of orange to brown fluorescing alginite and sporinite macerals are also observed brecciated between grains together with hydrocarbon fluid inclusions. The deepest core sample analyzed from the Hart River Formation (146/10) contains a framboidal pyrite-rich siltstone matrix with trace amounts of solid, non-fluorescing, isotropic primary and secondary migrabitumen. Associated hydrocarbon fluid inclusions are also observed trapped within intracrystalline growth zones and microfractures. Trace amounts of mostly amorphous stylocumulates and granular amorphinite kerogen with framboidal pyrite inclusions are also found between intergranular pore spaces. In addition, sample 256/13 and 257/13 suggest possible intrusion hydro thermal fluid and saddle dolomite. Allochthonous terrestrial plant derived organic macerals such as inertodetrinite are also found in all the samples but at very low concentrations (Type II/III kerogen by source).

S. Tuttle N-05 well

The data for this well (Figure 12; Table 5) consist of five new analyses (2 core, 3 cuttings) and 23 older data from Link (1988). The results from the new data are virtually identical to Link's older data which show that these near surface rocks reached the oil window with thermal maturity approaching 1.0 %Ro. Both sets of results indicate that below approximately 1000 m depth the thermal maturity increases into the wet gas and condensate stage. The results also indicate that the peak oil generation maturity stage is reached in the Upper Devonian strata (Imperial Formation).

Upper Imperial Formation (05/09, 06/09, 07/09)

The Upper Devonian strata are composed primarily of sandstone and carbonate shale with rare amounts of weak fluorescing mainly unicellular alginite macerals and small lenses of mostly allochthonous vitrinite macerals (Type II kerogen by source). Fluorescing hydrocarbon fluid inclusions are observed trapped within quartz grains. Vitrinite reflectance measurements range from 0.72 %Ro in the shallowest samples (21 m) to 1.20 %Ro in the deeper sample (1003 m), indicating a steep gradient that begins in the peak oil generation stage and rapidly approaches the wet gas window.

Lower Imperial Formation (03/09)

In the Upper Devonian strata near the Imperial-Canol contact, the lithology is composed of a mixture of siltstone, dolomite, pyrite-rich shale and calcite within a calcium carbonate matrix. The siltstone and shale contain some long, thin lenses of alginite-derived vitrinite macerals. The medium-grained calcite and dolomite contain micrinite-rich amorphous bitumen lenses within intergranular pores whereas small kerogen inclusions (<5 microns) are observed brecciated within the calcium carbonate.

Ogilvie Formation (04/09)

The Middle Devonian strata consist of very organically-lean and pyrite-rich limestone carbonates. The pyrite is found in both crystal and framboidal form. The reflectance value measured from the deepest sample is 1.40 %Ro which indicates thermal maturity in the wet gas stage. Though based on a single measurement, this %Ro value is within the range of the Link data.

N.Parkin D-61 well

The data from this well (Figure 13; Table 6) are from three core and 30 cuttings samples to a depth of 2277m. This entirely new set of data has an organic maceral assemblage dominated by amorphous kerogen and mostly reworked dispersed organic matter. There are also minor to trace amounts of fluorescing liptinite macerals. This well has a slightly steep maturity gradient that reaches the peak oil window at approximately 2000 m depth. Of the 26 samples that fall within the oil window, five are in Late Devonian (Frasnian) strata with vitrinite reflectance between 0.7-0.95 %Ro, which is within the peak oil generation window. The tops of the Ford Lake and Imperial/Tuttle formations in this well were determined using new biostratigraphy (Lane et al., 2012).

Burnthill Creek Formation (114/09, 115/09)

Two Upper Cretaceous samples from the Burnthill Creek Formation display a highly reworked host matrix dominated by siltstone and very fine-grained sandstone with organic maceral assemblages consisting of granular brown hebamorphinite, allochthonous vitrinite and inertinite macerals (some of the reworked macerals have high %Ro) brecciated between intergranular pores. Fluorescing liptinite macerals include sporinite (yellow to orange) and a bituminite matrix (granular brown). Samples from the shallow immature Cretaceous strata have an average vitrinite reflectance of approximately 0.48 %Ro.

Parkin Formation (110/09 to 112/09, 116/09)

In the upper part of the Cretaceous Parkin Formation (116/09) results are similar to those from the Burnthill Creek Formation, however rare hydrocarbon fluid inclusions are observed in quartz and calcite minerals. Three core samples (110/09 to 112/09) from lower in the Parkin Formation are mainly carbonate shale with fluorescing and non-fluorescing sporinite and alginite macerals, and minor framboidal pyrite inclusions. A few granular, brown hebamorphinite macerals in intergranular pores and allochthonous vitrinite and inertinite macerals are also observed. The deepest of the three samples (324.6 m) contains liptinite macerals and pyrite-rich shale with some oil staining between the intergranular pores of coarse-grained sandstone. Fluoramorphinite matrix with bright fluorescing alginite inclusions is also present. These thermally immature core samples have an average vitrinite reflectance of 0.49 %Ro, however this may be partially suppressed due to surface staining by soluble organics. Figure 14 shows six photomicrographs from sample 112/09 (324.6 m) displaying sporinite, vitrinite and alginite macerals (Type II/III kerogen by source).

Ford Lake Formation (117/09 to 128/09)

This formation can be divided into two major parts (upper and lower) based on the distinct variation in lithotype. The upper Ford Lake Formation (117/09 to 120/09) shows a mainly reworked matrix of silt, shale and sandstone (some displaying partial diagenetic dolomitization). Dispersed organic matter includes non-fluorescing sporinite, rare yellow fluorescing unicellular alginite macerals and mostly allochthonous vitrinite and inertinite (fusinite and inertodetrinite) macerals (Type II/III kerogen by source). Three samples (118/09, 119/09, 120/09) also contain non-fluorescing hebamorphinite lenses and liptinite macerals consisting mainly of sporinite (some pollen) and small, thin-walled unicellular

prasinophyte alginite associated with non-dolometized shale and very fine sandstone. High percentage of yellow fluorescing migrated bitumen between intergranular pores and fractures of sandstone matrix are also common in these samples. Bright yellow fluorescing hydrocarbon fluid inclusions are found trapped within calcite and quartz minerals in all three samples. The lower sections of this formation, samples 121/09 to 128/09 are dominated by silty shale matrix, with rare carbonate and sandstone present. Yellow to reddish-brown fluorescing and non-fluorescing sporinite (mostly brecciated within a siltstone matrix), small yellow-fluorescing unicellular, thin-walled alginite macerals and networks of hebamorphinite are also observed. A notably high input of allochthonous detrovitrinite and inertinite (some fusinite but mostly inertodetrinite) macerals is present in all three samples. Granular grey solid bitumen, large pyrite minerals (126/09-127/09), rare hydrocarbon fluid inclusions trapped within calcite and quartz minerals, and little dolomite matrix are also observed. Vitrinite reflectance values in the samples taken from these Carboniferous strata are between 0.45-0.58 %Ro indicating immature to marginal thermal maturity.

Imperial/Tuttle Succession (129/09 to 140/09)

Samples from the upper Imperial/Tuttle Succession (129/09 to 136/09) show sporinite- and pyrite-rich siltstone and carbonate shale containing mostly small, fluorescing, thin-walled unicellular alginite and granular brown lenses of non-fluorescing networks of hebamorphinite including rare sporinite macerals. Rare granular, grey isotropic solid bitumen and yellow fluorescing asphaltine-like bituminite macerals are also observed between pores and fractures of the dolomitized sandstone matrix including hydrocarbon fluid inclusions within calcite and quartz minerals and carbonate fractures. A high input of allochthonous detrovitrinite and inertinite (mostly inertodetrinite and some semifusinite and fusinite) macerals are found throughout the formation (Type II/III kerogen by source). Figure 15 shows six photomicrographs from sample 133/09 (1609.3 m) displaying alginite, vitrinite, sporinite and hebamorphinite macerals. Rare large pyrite minerals and dolomite matrix are also observed. Deeper in the Imperial/Tuttle succession (137/09 to 140/09), fine to very-fine sandstone matrix becomes dominant. The organic matter assemblages shift from non-fluorescing bitumen and hydrocarbon fluid inclusions within calcite and quartz to rare orange fluorescing sporinite (within intergranular pores) displaying higher reflecting vitrinite macerals and non-fluorescing granular amorphous kerogen with rare dark brown, finely dispersed hebamorphinite matrices. Reflectance values range from 0.57 - 0.73 %Ro which indicates that the maturity values for all samples from this formation have reached the oil window and the deeper samples with higher %Ro have reached the

peak oil generation stage (Figure 13; Table 6). The dispersed organic matter assemblage of the lower section of Imperial Formation is also considered as Type II/III kerogen by source.

Imperial – Canol boundary samples (140/09, 141/09)

Near the Imperial – Canol boundary the samples are dominated by organically lean carbonate shale interbedded with framboidal and crystalline pyrite-rich shaly microlithotypes with minor contributions from non-fluorescing, small organic matter mostly derived from unicellular alginite-like prasinophyte and sporinite macerals (Type II kerogen by source). There is fine to coarse grained sandstone with some brown, granular amorphous kerogen, rare thick coaly lenses and brown lenses of non-fluorescing alginite brecciated within intergranular pores and some dolomitized siltstone matrix.

Canol Formation samples (142/09, 143/09, 109/09, 113/09)

The Canol Formation samples consist of two pyrite-rich shaly siltstone matrix with minor amount of granular hebamorphinite lenses (142/09-143/09), rare small high reflecting vitrinite lenses, as well as carbonate shale with some yellow to non-fluorescing alginite and rare orange fluorescing sporinite macerals. Minor low reflecting siltstone with some yellow to orange fluorescing sporinite is present, possibly due to caving. Vitrinite reflectance data are highest in this part of the well with reflectance values of 0.80-0.95 %Ro, indicating thermal maturity within the peak oil generation window. Near the Canol-Ogilvie boundary, the two additional samples of organically lean limestone matrix (109/09, 113/09) show rare amount of pyrite-rich yellow to orange fluoramorphinite with small yellow fluorescing alginite within fractures and pore spaces of (Type II kerogen by source). Degraded granular solid bitumen proximal to the edge of the matrix and rare hydrocarbon fluid inclusions are also observed within calcite, saddle dolomite and minerals brecciated within a dolometized limestone matrix. No vitrinite-like macerals are present to obtain reflectance values; therefore these two samples are not included on the plots.

Blackstone D-77 well

The data from this well (Figure 16; Table 7) includes eight new analyses (3 core, 5 cuttings) and 37 older analyses from Link (1988). The new data represent measured average %Ro of indigenous vitrinite macerals, and vitrinite-equivalent reflectance of solid bitumen in the absence of vitrinite macerals. The measured solid bitumen %Ro is converted to vitrinite equivalent using the Jacob (1989)

equation. The new set of data, though limited in number of samples, extend to the Silurian Road River Group as compared to Link data that only extend to the Devonian Canol Formation.

The maturity gradients from Link (1988) and the new data are very similar particularly in the Carboniferous and Lower Permian strata where there are numerous data. The slight disagreement between the average %Ro values is most likely due to the possible inclusion of measured values of solid bitumen macerals in the calculation and interpretation of the Link data. In general, inclusions of less thermally mature caved and more mature reworked organic macerals may decrease or increase both the average and the standard deviation of the sample being analyzed. The results from Link (1988) indicate that the Permian Jungle Creek Formation reached the peak oil generation window. All of the remaining samples from the Carboniferous formations are at maturity values equivalent to the late oil-to-wet gas generation windows (1.0 to 1.8 %Ro).

Blackie, Hart River and Ford Lake formations (246/09 to 249/09)

The organic maceral assemblages of these samples from Carboniferous and Lower Permian strata are dominated by organic-rich black shale made up of mostly interconnected networks of pyrite-rich amorphous kerogen and amorphinite lenses with minor amounts of vitrinite and solid bitumen inclusions. Sulphide-rich phosphatic nodules and rare siliceous microfossils are observed in some matrices. Weak orange to brown fluorescing alginites are also found in Blackie Formation, which is within the range of fluorescence colour properties for average measured thermal maturity of 1.02 %Ro (Potter, 1998). The Hart River (247/09) and two Ford Lake samples (248/09 and 249/09) have an average thermal maturity of 1.25, 1.33 and 1.60 %Ro (Table 7), respectively. These organic rich black shales consist mostly of amorphous kerogen with high amount of framboidal pyrite inclusions with minor presence of some limestone matrix. Some carbonate matrix from sample 149/10 show evidence of oil migration.

Ogilvie Formation (250/09 and 243/09)

The organic matter assemblages of the samples consist mainly of organic-rich black shale with interconnected networks of pyrite-rich granular amorphous kerogen showing minor amounts of phosphatic nodules and rare siliceous and chitinous microfossils (Type I kerogen by source). An organically lean limestone matrix with isotropic and granular migrabitumen brecciated between

intergranular pores and microfractures is also observed. The average reflectance of this sample is 1.78 %Ro, which is within the dry gas window.

This sample has an organic-rich carbonate limestone and dolomite matrix consisting of mostly migrated isotropic, pitted, over-mature pyrobitumen brecciated between intergranular pores and fractures. A minor amount of granular networks of amorphous kerogen with framboidal pyrite inclusions is also observed in the some of the limestone matrix (Type I kerogen by source). The average vitrinite equivalent reflectance ($\%Ro_{eqvt}$) of this formation is 2.28 %Ro, which places it in the dry gas window. Figure 17 shows six photomicrographs displaying solid bitumen and migrated pyrobitumen macerals, as well as devolatilization vacuoles resulting from thermal cracking. The thermal cracking may be due to the thermal effects of hydrothermal fluid migration (dolomite minerals) through the carbonate succession.

Road River Group (244/09, 245/09)

These two shaly samples have similar organic matter assemblages consisting of mostly interconnected networks of pyrite-rich amorphous kerogen with minor to rare amounts of measurable vitrinite-like macerals derived from unicellular algae or colonial alginite similar to *Gloeocapsomorpha. prisca* (Type I kerogen by source). Most of the measured particles of dispersed organic matter are isotropic pyrobitumen (some showing devolatilization vacuoles) with reflectance values of 3.7 %Ro and vitrinite equivalent values of 2.70 $\%Ro_{eqvt}$, This %Ro equivalent is within the range of the small number of vitrinite like macerals measured (2.68 and 2.70 %Ro, respectively). Trace amounts of phosphatic nodules and siliceous microfossils are also observed in the matrix. The similarity between the thermal maturities of the Ogilvie Formation samples (243/09) suggests that they were subjected to the same level of heating. The kerogen assemblages and thermal maturity of the Road River Group suggests that it may be the source of the migrated pyrobitumen observed in the Ogilvie Formation above.

Beaver G-01 well

The data from this well (Figure 18; Table 8) includes five core and 17 cuttings samples over a depth of 4500 m. At surface, thermal maturity is close to, or at, the start of the oil window passing into early gas generation in the 1500-2000 m depth range. Below approximately 500 m, the maturity appears to show a consistent increase with depth with little variation from the trend. Almost all of the data from

the Carboniferous to Cretaceous strata plot within the oil window with three data points (Mattson and Fantasque formations) showing a thermal maturity within the peak oil generation window.

Toad Formation (116/10-118/10)

These samples were taken near the Garbutt-Toad unconformity and just above the Fantasque Formation. The lithology is represented by siltstone, shale, sandstone and rare dolomite matrices. Dispersed organic matter (DOM) assemblages are also dominated by allochthonous vitrinite and inertinite (fusinite and inertodetrinite) macerals with rare amounts of orange fluorescing sporinite, granular brown fluorescing bituminite, yellow fluorescing alginite and orange fluorescing liptodetrinite macerals. The absence or lack of autochthonous organic macerals makes it difficult to estimate the true %Ro. Trace amounts of non-fluorescing sporinite and alginite derived macerals were also observed. The kerogen is Type II/III by source.

The fluorescence properties suggest a much lower thermal maturity (~ 0.50-0.80 %Ro) than the measured average vitrinite reflectance of >1.10 %Ro and higher. The DOM assemblages and the wide range of vitrinite reflectance values of these samples suggest that the bulk of the organic material in this formation is recycled from older and more thermally mature sediments.

Fantasque Formation (119/10 to 120/10)

The upper Fantasque sample (119/10) contains mostly a reworked matrix of carbonate-shale and siltstone (some intergranular pores and fractures showing partial dolomitization) with some allochthonous vitrinite and inertinite (large fusinite and inertodetrinite) macerals and non-fluorescing granular hebamorphinite lenses (Type II/III kerogen by source). The organic maceral assemblage of this sample indicates a high input of reworked older and thermally mature matrix (>0.89 %Ro, not included in the table) similar to the three overlying samples. However, there are measured collotelinite macerals that are representative of the autochthonous population and are within the range (yellow to orange) of the observed fluorescence properties of the liptinite maceral.

The organic-rich carbonate shale (120/10) shows minor amounts of yellow fluorescing prasinophyte (*Leiosphaeridia* sp., and *Tasmanites* sp.) alginite, spiny marine acritarch, and orange fluorescing sporinite macerals (Type II kerogen by source). Rare amounts of orange to non-fluorescing bitumen macerals, phosphatic nodules and reworked inertinite and vitrinite macerals are all observed in the matrix. The reflectance value (0.67 %Ro) of this sample is within the peak oil generating window.

The organically lean siltstone sample from this formation (120/10) has an organic matter assemblage consisting of trace amounts of autochthonous marine acritarch. Some yellow fluorescing migrated bitumen (asphaltine) is found in intergranular pores and in quartz grain microfractures. This sample lies along the Fantasque-Mattson Formation boundary.

Mattson Formation (121/10 to 126/10)

These five samples are characterized by highly reworked strata with mostly reworked organic matter assemblages with the exception of the sample taken near the Fantasque-Mattson boundary (121/10). This sample has a maceral assemblage that is similar to sample 120/10, which is an organically lean siltstone consisting of trace amounts of autochthonous marine acritarch and possibly dinoflagellate alginite. Some yellow fluorescing migrated bitumen (asphaltine) and golden yellow fluorescing hydrocarbon fluid inclusions are also observed between intergranular pores and in quartz grain microfractures. Samples 123/10 to 126/10 are a sequence of carbonate shale, siltstone to very fine- to fine-grained sandstone with rare amounts of yellow to orange fluorescing liptinite macerals. The average reflectance ranges from 0.86 to 1.51 %Ro which is within the peak oil to wet gas condensate windows. There are mostly orange fluorescing sporinite and small, yellow fluorescing, thin-walled unicellular alginite and granular brown non-fluorescing networks of hebamorphinite matrix brecciated within a shaly matrix. A high input of allochthonous detrovitrinite and inertinite (some fusinite, mostly inertodetrinite) macerals is present along with granular grey solid bitumen (Type II/III kerogen by source) and large pyrite crystals. Trace amounts of hydrocarbon fluid inclusions are observed within calcite and quartz minerals, and a dolomite matrix. There is also evidence of dolomitization (diagenetic?) in some microfractures which may be associated with a possible increase in the thermal maturity of the kerogen matrix and primary bitumen. This may account for the low and high reflecting secondary bitumen, particularly in samples 125/10 and 126/10 (1.51 %Ro).

Besa River, (127/10 to 129/10)

The organic matter assemblage of these organically lean carbonate shale samples consist mostly of allochthonous terrestrial plant-derived vitrinite and inertinite (fusinite) macerals along with autochthonous alginite-derived collotelinite and migrabitumen macerals (Type II/III kerogen by source). There is some evidence of dolomitizing hydrothermal fluid intrusion in some matrices that may increase the thermal maturity of the affected isotropic primary and secondary low and high reflecting isotropic solid bitumen. Soluble fracture-filling yellow-fluorescing bitumen is present and is

most likely derived from younger source rock, from caved materials or from contamination. This may be a reason that many of the Tmax values are suppressed.

Kotcho Formation (352/09 to 355/09 - core and 130/10 - cuttings)

The four core samples taken from the Kotcho Formation consist of amorphinite-rich black shale with mainly small lenses of vitrinite macerals derived from unicellular alginite such as prasinophyte and rare solid bitumen (mainly granular). The average vitrinite reflectance values (2.24 to 2.46 %Ro) of the core samples are mostly within the standard deviation of one another as well as that of the cuttings sample (2.40 %Ro). Minor to rare amounts of both siliceous and chitinous microfossils are also present. The main difference between the core and cutting samples is the uniformity of the microlithotypes observed in the core as compared to the cuttings which cave from younger formations.

Fort Simpson and Muskwa formations (131/10 and 132/10)

The Fort Simpson Formation is organically rich black shale dominated by interconnected networks of granular amorphous kerogen derived from matrix bituminite and alginite (Type II kerogen by source). Also observed are granular primary isotropic pyrobitumen (3.15 %Ro) brecciated between dolomite minerals. Some bitumen matrices show anisotropy, which is a result of thermal cracking of solid bitumen producing dry gas. Other matrices show evidence of sulphide enrichment with high micrinite and pyrite inclusions. Organically lean shale microlaminates are also observed between organic rich laminates, possibly due to marine regression and transgression.

The Muskwa Formation sample (132/13) is a carbonate shale rich matrix with both granular and anisotropic pyrobitumen mostly associated with limestone and minor amounts of amorphous kerogen associated with a shaly stylocumulates matrix brecciated within the intergranular pore spaces. Most of the measured %Ro values are for high and low reflecting isotropic pyrobitumen.

Nahanni Formation (356/09)

The core sample from the Nahanni Formation consists of a limestone/dolomite matrix with mostly overmature isotropic and granular pyrobitumen (rare thermally cracked anisotropic pyrobitumen) macerals and rare stylocumulate lenses brecciated between intergranular pores and fractures. Poor polish may have suppressed vitrinite reflectance measurement.

Summary/Conclusions

Since the seminal work of Link and Bustin (1989), little systematic analysis of thermal maturity has been carried out in Eagle Plain. Since 2009, the GEM Yukon Basins Project has acquired over 100 new organic petrology/vitrinite reflection data in conjunction with organic geochemistry and biostratigraphy as part of a larger study of the basin's evolution and petroleum systems. Recycling of organic matter is ubiquitous in the basin; and cuttings samples present the risk of caving. Nonetheless, several patterns are evident in the data, basinwide.

The results of vitrinite reflectance analysis show that most of the Upper Devonian to Lower Cretaceous strata (Whitestone River, Imperial, Tuttle, Blackie, Hart River and Canol formations) reached the early stage of oil generation (>0.5 %Ro) or are at maturity levels equivalent to the oil generating window (0.70-1.30 %Ro) with the exception of the Blackstone D-77 well located in the southernmost part of the basin, which reaches the wet to dry gas window (>1.30 %Ro) in Carboniferous strata. The high thermal maturity of the Blackstone D-77 well as compared to the other wells can be attributed to deeper burial depths but is possibly due to the hydrothermal anomalies observed in the Ogilvie Formation, which shows evidence of dolomitization and thermal cracking.

Thick sections of the Hope N-53, Ellen C-24 and Shaeffer Creek O-22 wells attained the peak oil generating window (0.70 to 1.00 %Ro) including a thick section of the Whitestone River Formation in N. Hope N-53 well. These results support the initial Link and Bustin (1989) study, which showed similar results.

%Ro values for the Canol Formation range between ~0.8% (N. Parkin D-61) to ~1.8% (Blackstone D-77) in wells that encountered this unit. In nearly all wells, mid-Cretaceous strata are within the oil window (Ro>0.5%). However, most of the samples from the Cretaceous units for both Ellen C-24 and Shaeffer Creek O-22 wells are immature (<0.50 %Ro) or in the biogenic gas window. None of the wells shows a thermal discontinuity at the sub-Mesozoic unconformity, demonstrating that the thermal peak post-dates mid-Cretaceous time throughout the basin. At the sub-Mesozoic unconformity, vitrinite reflectance varies from ~0.4% in several wells, up to ~1.0% (N. Hope N-53); but there appears to be little correlation between thermal maturity and present burial depth. This is consistent with previous interpretations (e.g., Link and Bustin, 1989) and with interpretations of early Tertiary tectonic exhumation of the range (e.g., Lane, 1998).

Photomicrographs show the observed dispersed organic matter in the various microlithotypes. The kerogen type by source is dominated by Type II and Type II/III of mostly marine depositional environment.

Acknowledgements

The authors are indebted to Richard Fontaine, at the GSC core and sample facility, students Adam Hayman and Lindsay Kung for assistance with sampling, Dale Issler for critical review, Krista Boyce for editing the revision files and Denise Then for assisting with final document preparation.

References

Bustin, R.M., Cameron, A.R., Grieve, D.A., and Kalkreuth, W., 1983. Coal petrology: Its principles, methods and applications, short course notes 3; Geological Association of Canada, 230 p.

Cameron, A. R., Potter, J., and Goodarzi, F., 1994. Coal and oil shale of Early Carboniferous age in northern Canada: significance for palaeoenvironmental and palaeoclimatic interpretations; Palaeogeography, Palaeoclimatology and Palaeoecology, v. 106, p. 135-155.

Chow, N., Wendte, J. and Stasiuk, L.D. 1995. Productivity versus preservation controls on two organic-rich carbonate facies in the Devonian of Alberta: sedimentological and organic petrological evidence. Bulletin of Canadian Petroleum Geology, v. 43, p. 433–460.

Cole, G.A., Abu-Ali, M.A., Aoudeh, S.M., Carrigan, W.J., Chen, H.H., Colling, E.L., Gwathney, W.J., Al-Hajji, A.A., and Halpern, H.I., 1994. Organic geochemistry of the Paleozoic petroleum system of Saudi Arabia; Energy Fuels, v. 8, p. 1425-1442.

Demaison, G. J. and Moore, G. T., 1980. Anoxic environments and oil source bed genesis; American Association of Petroleum Geologists Bulletin, v. 64, p. 1170-1209.

Dixon, J. 1992. Stratigraphy of the Mesozoic Strata, Eagle Plain area, northern Yukon. Geological Survey of Canada Bulletin 408, 58p.

Dixon, J. 1998. Permian and Triassic Stratigraphy of the Mackenzie Delta, and the British, Barn and Richardson mountains, Yukon and Northwest Territories; Geological Survey of Canada Bulletin 528, 46p.

Dorning, K.J. 1987. The organic paleontology of Palaeozoic carbonate environments. In: Micropaleontology of Carbonate Environments. Hart, M.B. (ed.). Ellis Horwood, Chichester, p. 256–265.

Dow, W. G., 1977. Kerogen studies and geological interpretations; Journal of Geochemical Exploration, v. 7, p. 79-99.

Fallas, K.M. 2006: Geology, Mount Martin, Yukon Territory–Northwest Territories–British Columbia; Geological Survey of Canada, Map 2087A, scale 1:50 000.

Fraser, T. and Hogue, B. 2007. List of Wells and Formation Tops, Yukon Territory, version 1.0; Yukon Geological Survey, Open File 2007-5. http://www.geology.gov.yk.ca

Haggart, J.W., Bell, K.M., Schröder-Adams, C.J., Campbell, J.A., Mahoney, J.B. and Jackson, K.W. 2013. New biostratigraphic data from Cretaceous strata of the Eagle Plain region, northern Yukon: Reassessment of age, regional stratigraphic relationships, and depositional controls. Journal of Canadian Petroleum Geology, v. 61 (2), p. 101-132.

Huc, A. Y., 1988. Sedimentology of organic matter; *in* Humic substances and their role in the environment, (ed.) F.H. Frimmel and R.F. Christman; Dahlem Konferenzen, John Wiley, p. 215-243.

Huc, A. Y., 1990. Understanding organic facies: A key to improved quantitative petroleum evaluation of sedimentary basins; *in* Deposition of organic facies, (ed.) A.Y. Huc; AAPG Studies in Geology 30, p. 1-12.

International Committee for Coal Petrology, 1975. Handbook of coal petrology Centre Nationale de la Recherche Scientifique, Paris, (second supplement to second edition).

International Committee for Coal Petrology, 1995. Vitrinite classification, ICCP System 1994. Aachen, Germany, 24 p.

Jackson, K., 2012. Mid- to Late Cretaceous stratigraphy, sedimentology and hydrocarbon potential, Eagle Plain Basin, northern Yukon; MSc thesis, University of Calgary, Calgary, Canada, 194 p.

Jackson, K.W., McQuilkin, M., Pedersen, P.K., Lane, L.S., and Meyer, R. 2011. Preliminary observations on stratigraphy and hydrocarbon potential of Middle to Upper Cretaceous strata, Eagle Plain Basin, northern Yukon. *In:* Yukon Exploration and Geology 2010, K.E. MacFarlane, L.H. Weston and C. Relf (eds); Yukon Geological Survey, p. 125-134.

Jacob, H., 1989. Classification, structure, genesis and practical importance of natural solid oil bitumen ("migrabitumen"); International Journal of Coal Geology, v. 11, p. 65-79.

Jones, A.L. and Gal, L.P., 2007. Northwest Territories oil and gas poster series: Basins & petroleum resources, table of formations, schematic cross sections; Northwest Territories Geoscience Office, NWT Open File 2007-03.

Lane, L.S., 1998. Late Cretaceous-Tertiary evolution of northern Yukon and adjacent Arctic Alaska; American Association of Petroleum Geologists Bulletin, v. 82, p. 1353-1371.

Lane, L.S. 2007. Devonian - Carboniferous Paleogeography and Orogenesis, northern Yukon and adjacent Arctic Alaska. Canadian Journal of Earth Sciences, v. 44, No. 5, p. 679-694.

Lane, L.S., and Dietrich, J.R. 1995. Tertiary structural evolution of the Beaufort sea - Mackenzie Delta region, Arctic Canada. Bulletin of Canadian Petroleum Geology, v. 43, p. 293-314.

Lane, L.S., Hayman, A., Utting, J., and Sweet, A.R., 2012. Summary of current

geochemical, geophysical and biostratigraphic data for Chevron SOBC WM N. Parkin YT D-61 (UWI 300D616630137000), Eagle Plain, Yukon; Geological Survey of Canada, Open File 7050, 1 CD-ROM. doi:10.4095/290117.

Leythaeuser, K. F. A., Hagemann, H. W., Hollerbach, R. W. T. H., and Schaefer, K. F. A., 1980. Hydrocarbon generation in source beds as a function of type and maturation of their organic matter as mass balance approach; *in* Origin, migration and accumulation of hydrocarbons, Proceedings 101 World Petroleum Congress, Heyden, London, v. 2, p. 31-41.

Link, C.M., 1988. A reconnaissance of organic maturation and petroleum source potential of Phanerozoic strata in northern Yukon and northwestern District of Mackenzie. M.Sc. thesis, University of British Columbia, Vancouver, Canada, 260 p.

Link, C. M. and Bustin, R. M., 1989. Organic maturation and thermal history of Phanerozoic strata in northern Yukon and northwestern District of Mackenzie; Bulletin of Canadian Petroleum Geology, v. 37, p. 266-292.

Mackowsky, M. –Th., 1982. Methods and tools of examination; *in* Stach's textbook of coal petrology, (ed.) E. Stach, M.-Th. Mackowsky, M. Teichmüller, G.H. Taylor, D. Chandra, and R. Teichmüller; Gerbruder Borntaeger, Berlin, p. 295-299 (third edition).

Morrow, D. W. 1999. Lower Paleozoic stratigraphy of northern Yukon Territory and northwestern District of Mackenzie; Geological Survey of Canada Bulletin 538, 202p.

Morrow, D.W., Jones, A.L., and Dixon, J, 2006. Infrastructure and resources of the northern Canadian mainland sedimentary basin. Geological Survey of Canada Open File 5152, 59 pages, doi:10.4095/222151..

Norris, D.K., 1984. Geology of the northern Yukon and northwestern District of Mackenzie. Geological Survey of Canada, Map 1581A, Scale 1:500,000

Osadetz, K.G. Zhuoheng Chen, Z. and Bird, T.D. 2005. Petroleum Resource Assessment, Eagle Plain Basin and Environs, Yukon Territory, Canada; Geological Survey of Canada Open File 4922.

Pigage, L., 2009. Yukon table of formations; Yukon Geological Survey and Oil and Gas Resources Branch, v. 32.

Potter, J., 1998. Organic petrology, maturity, hydrocarbon potential and thermal history of the Upper Devonian and Carboniferous in the Liard Basin, northern Canada; Ph. D thesis, Newcastle University, Newcastle upon Tyne, United Kingdom, 214 p.

Potter, J., Richards, B. C., and Cameron, A. R., 1993a. The petrology and origin of coals from the Lower Carboniferous Mattson Formation, southwestern District of Mackenzie, Canada; International Journal of Coal Geology, v. 24, p. 113-140.

Potter, J., Richards, B. C., Morrow, D. W., and Goodarzi, F., 1993b. The organic petrology and thermal maturity of Lower Carboniferous and Upper Devonian source rocks in the Liard Basin at Jackfish Gap-Yohin Ridge and North Beaver River, Northern Canada: Implications for hydrocarbon exploration; Energy Sources, v.15, p. 289-314.

Potter, J., Stasiuk, L. D.,Cameron, A. R., 1998. A petrographic atlas of the Canadian coal macerals and dispersed organic matter. Canadian Society for Caol Science and Organic Petrology. Calgary, Canada. 105 pages.

Powell, T. G. and Snowdon, L. R., 1983. A composite hydrocarbon generation model: Implications for evaluation of basins for oil and gas; Erdöl und Köhle, Erdgas, Petrochemie, v. 63, p. 163-169.

Richards, B.C., Bamber, E.W., and Utting, J., 1997. Upper Devonian to Permian. *In* The Geology, Mineral and Hydrocarbon Potential of Northern Yukon Territory and Northwestern District of Mackenzie. Geological Survey of Canada, Bulletin 422, p. 201-251.

Stasiuk, L. D., 1991. Organic petrology and petroleum formation in Paleozoic rocks of Northern Williston Basin, Canada; Ph. D. thesis, University of Regina, Regina, Canada, 312 p.

Stasiuk,L.D., 1999. Microscopic studies of sedimentary organic matter: key to understanding organic-rich strata, with Paleozoic examples from Western Canada. Geoscience Canada, v. 26, p. 149–172.

Stasiuk, L. and Fowler, M., 2004. Organic facies in Devonian and Mississippian strata of Western Canada Sedimentary Basin: Relation to kerogen type, paleoenvironment, and paleogeography; Bulletin of Canadian Petroleum Geology, v. 52, p. 234-255.

Tissot B. P. and Welte, D. H., 1984. Petroleum formation and occurrence; SpringerVerlag, Berlin, 699 p., (second revised and enlarged edition).

Tissot, B., Durand, B., Espitalie, J., and Combaz, A., 1974. Influence of nature and diagenesis of organic matter in petroleum generation; American Association of Petroleum Geologists Bulletin, v. 58, p. 499-506.

Tyson, R. V., 1987. The genesis and palynofacies characteristics of marine petroleum source rocks; *in* Marine petroleum source rocks. (ed.) J. Brooks and A.J. Fleet; Geological Society of London Special Publication 26, p. 47-67.

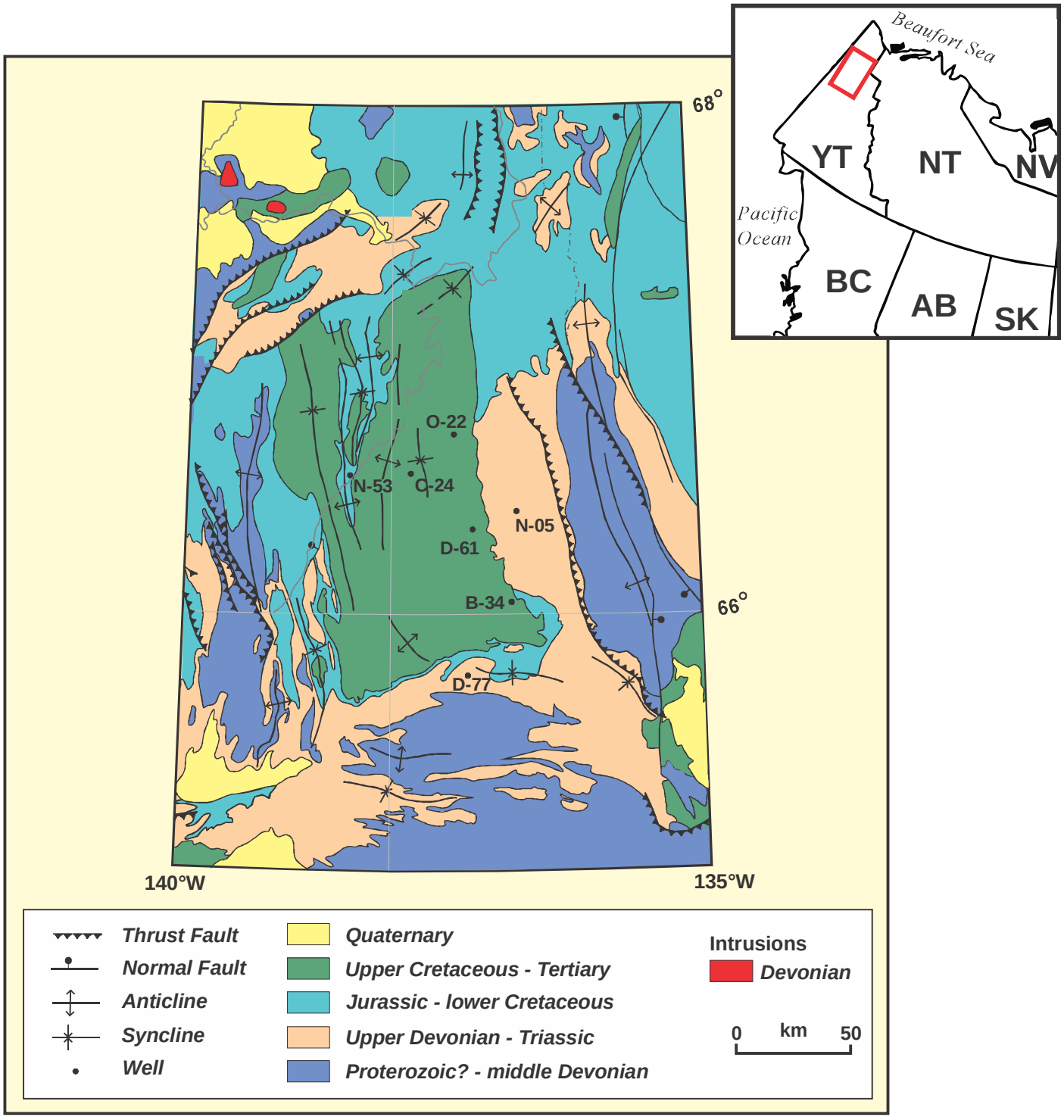

Figure 1: Map showin locations of the seven Eagle Plain wells included in the study. Simplified from Norris, 1984.

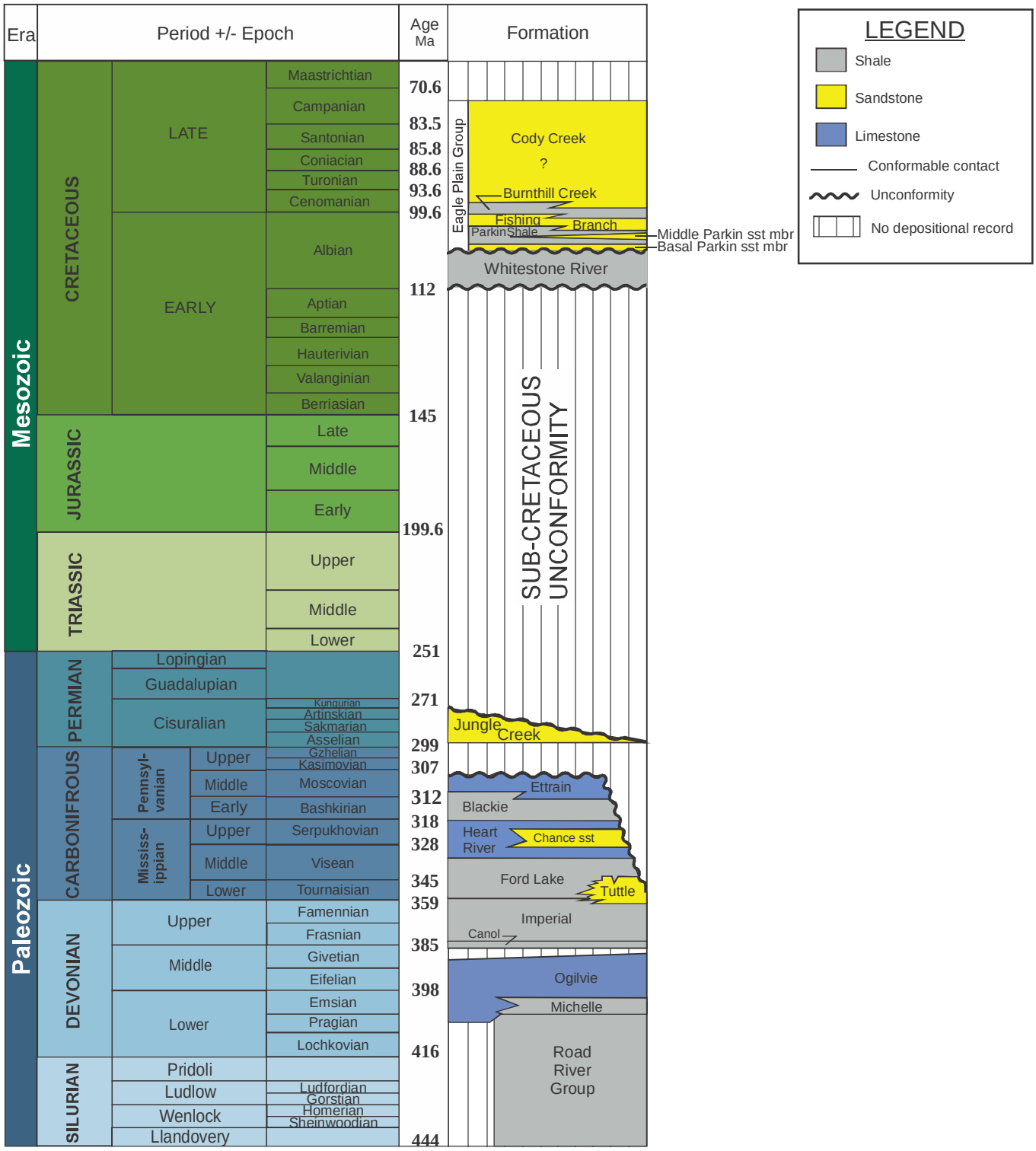

Figure 2: Stratigraphy of Eagle Plain Basin in northern Yukon (modified from Pigage, 2009 and Jackson, 2012)

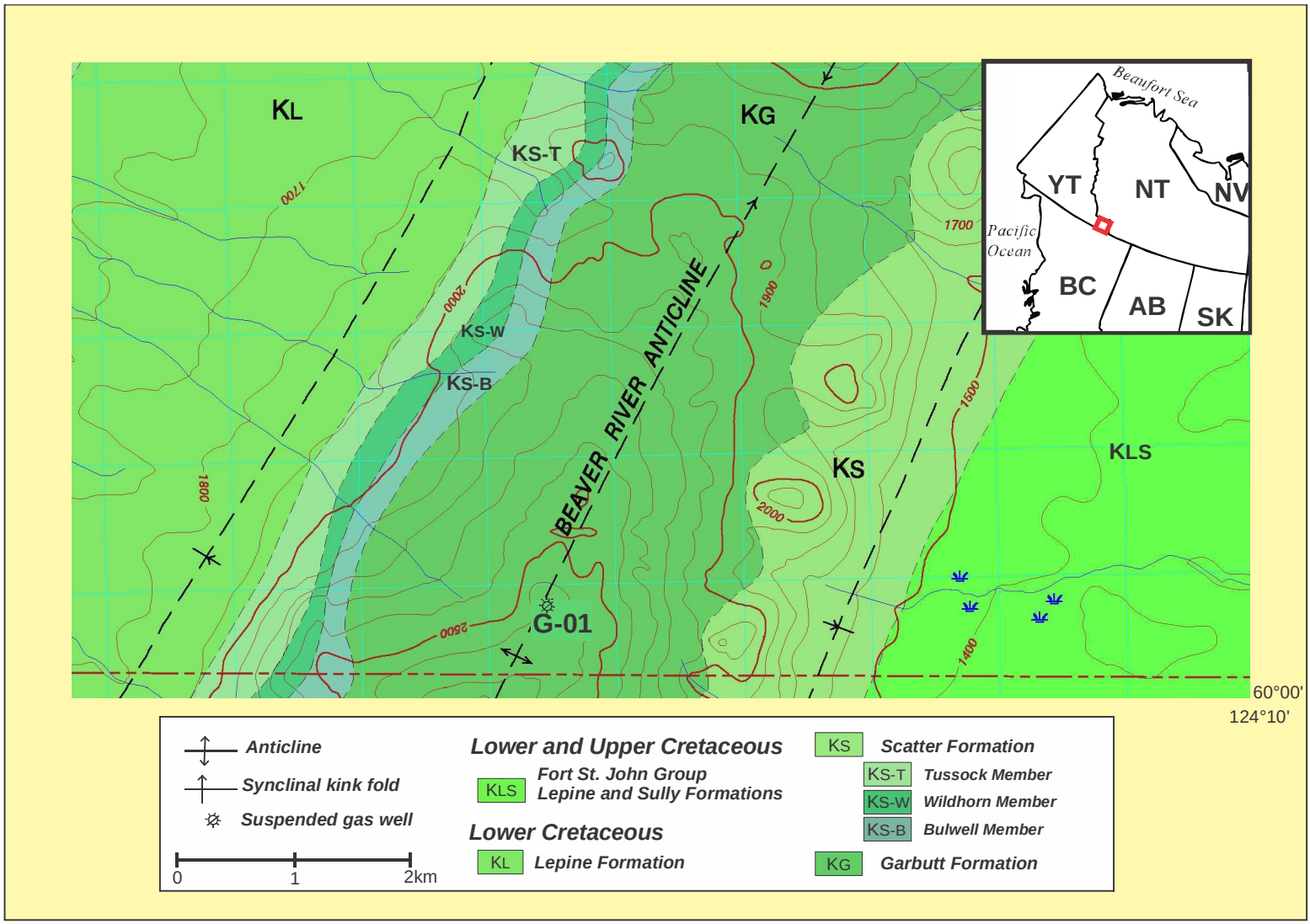

Figure 3: Map showing location of the Beaver G-01 well in Liard Basin Map 2087A (Fallas, 2006)

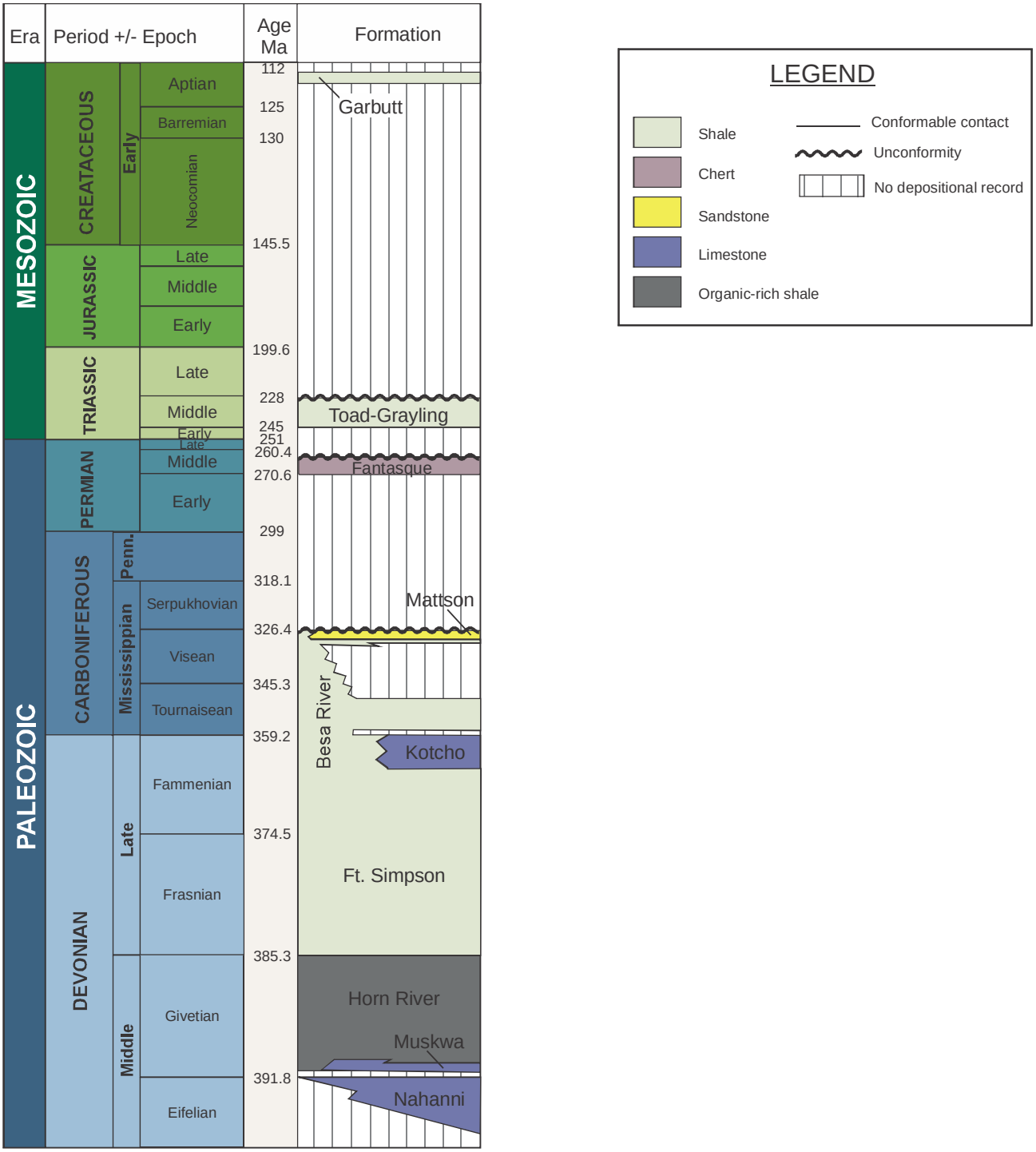

Figure 4: Stratigraphy of Liard Basin in south east Yukon (modified from Jones and Gal, 2007).

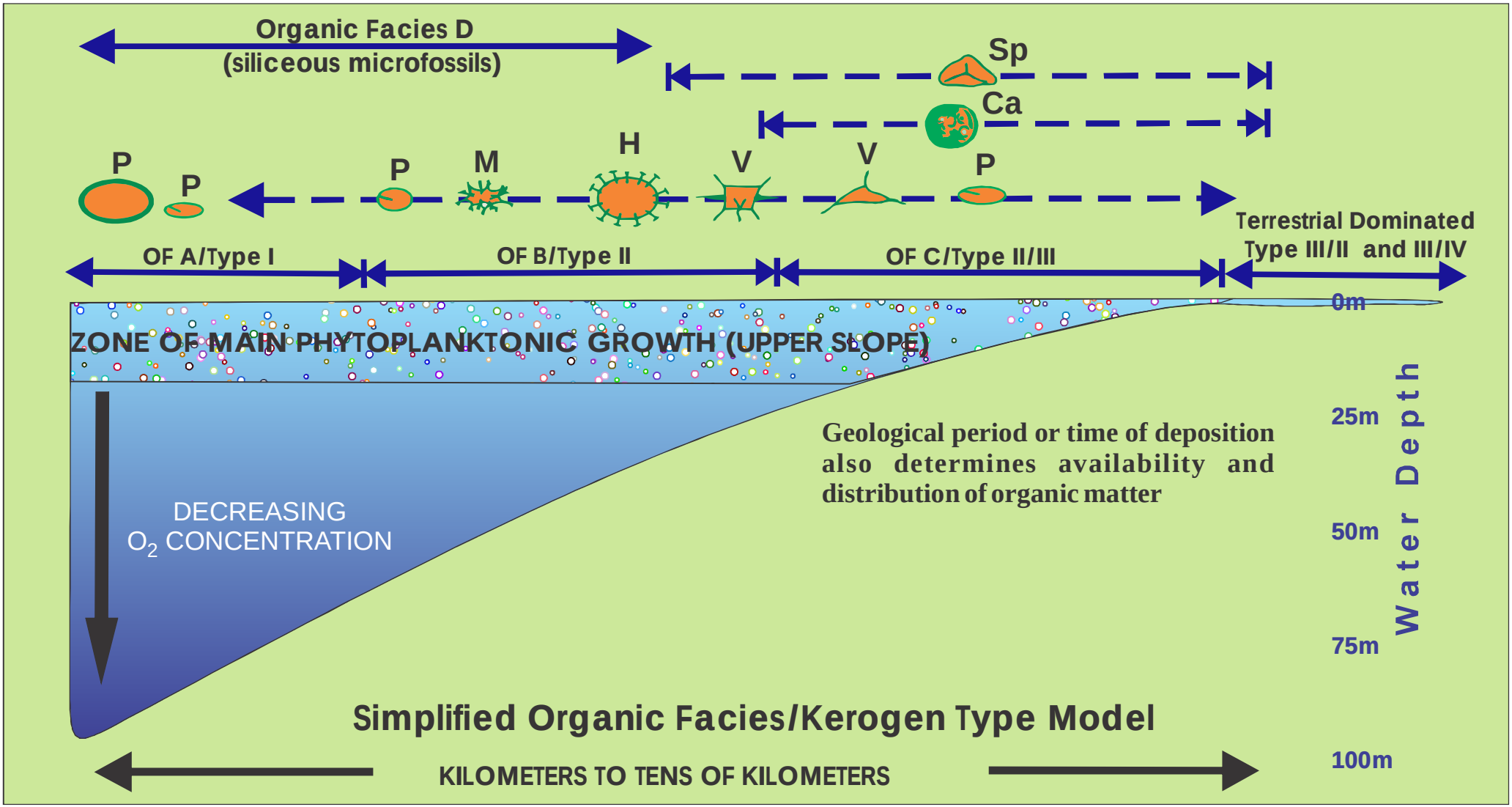

Figure 5 Simplified organic facies (OF)/kerogen type by source model for Eagle Plain Basin, Yukon, Canada base on observed dispersed organic matter (DOM). Organic facies A, B and C (Type I, II, II/III) is characterized by unicellular prasinophyte alginite (e.g. planktonic green microalgae, "P"), spiny acanthomorphic acritarchs (planktonic, green microalgae; "H, M, V", coccoidal alginite (planktonic green and/or blue green microalgae, "Ca") with minor to trace amount of input from terrestrial plant-derived macerals (i.e. spores "Sp"). Organic facies D is characterized by the deepest part of the basin where siliceous microfossils (mainly Radiolarian-derived) are most abundant. The presence of Radiolaria in the shallow end of the basin may be associated with areas of upwelling. Organic facies B and C(Type (II and II/III) are located in intermediate depths and shallow part of the shelf/platform region of the basin while OF A (Type I) represent the alginite rich deeper part of the basin. Period of marine regression and transgression also influenced the organic facies distribution in the basin. Geological period and temporal variation also determines organic facies and kerogen type. (Modified from Chow et. al., 1995 and Stasiuk and Fowler, 2004). See also Dorning, 1987; Tyson, 1987; and Stasiuk, 1999).

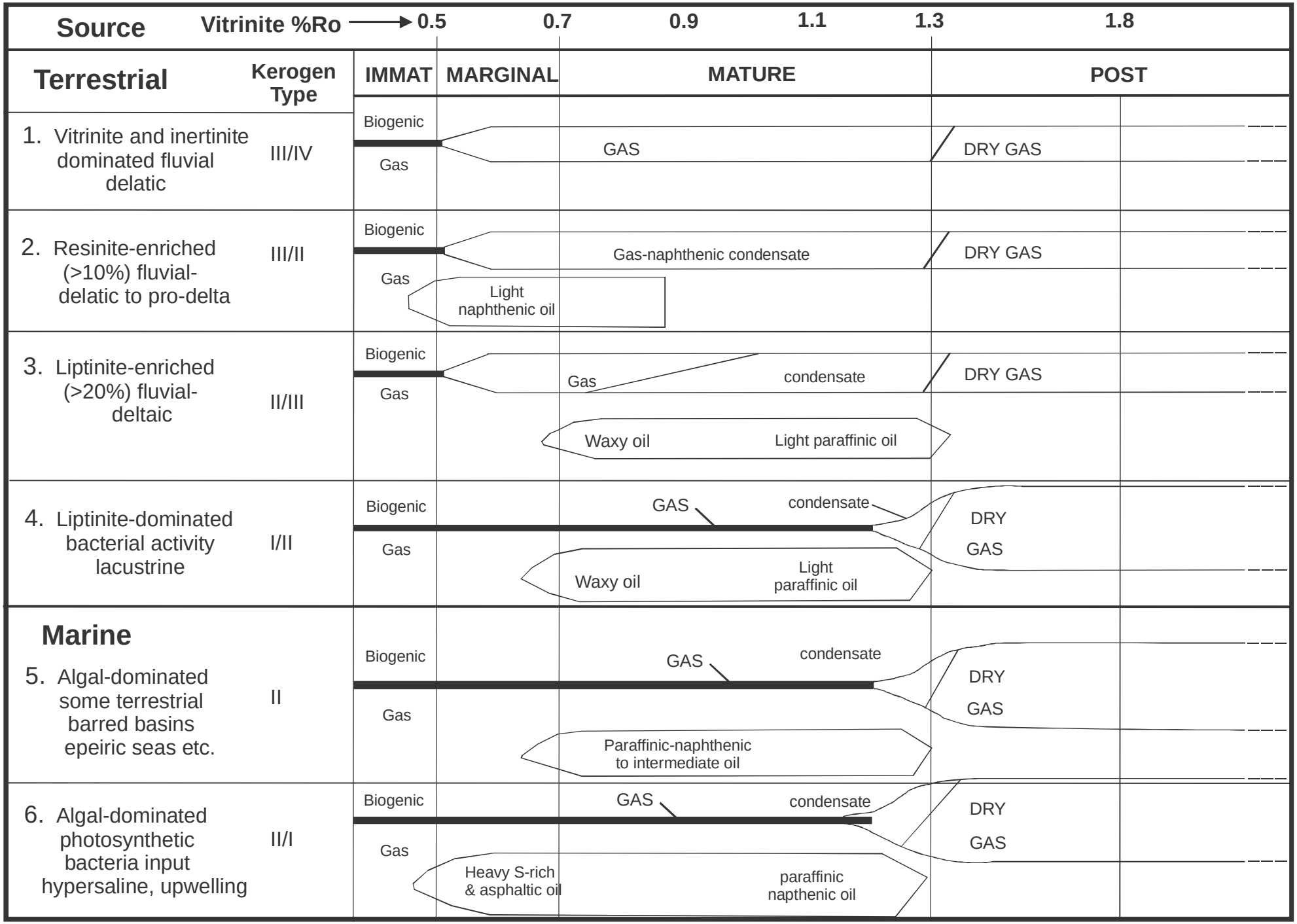

Figure 6. Hydrocarbon generation model. Vitrinite reflectance values can be used to determine form of hydrocarbon generated depending on source rock and kerogen type. (Modified from Potter, 1998 and Stasiuk, 1991 . See also Powell and Snowdon, 1983).

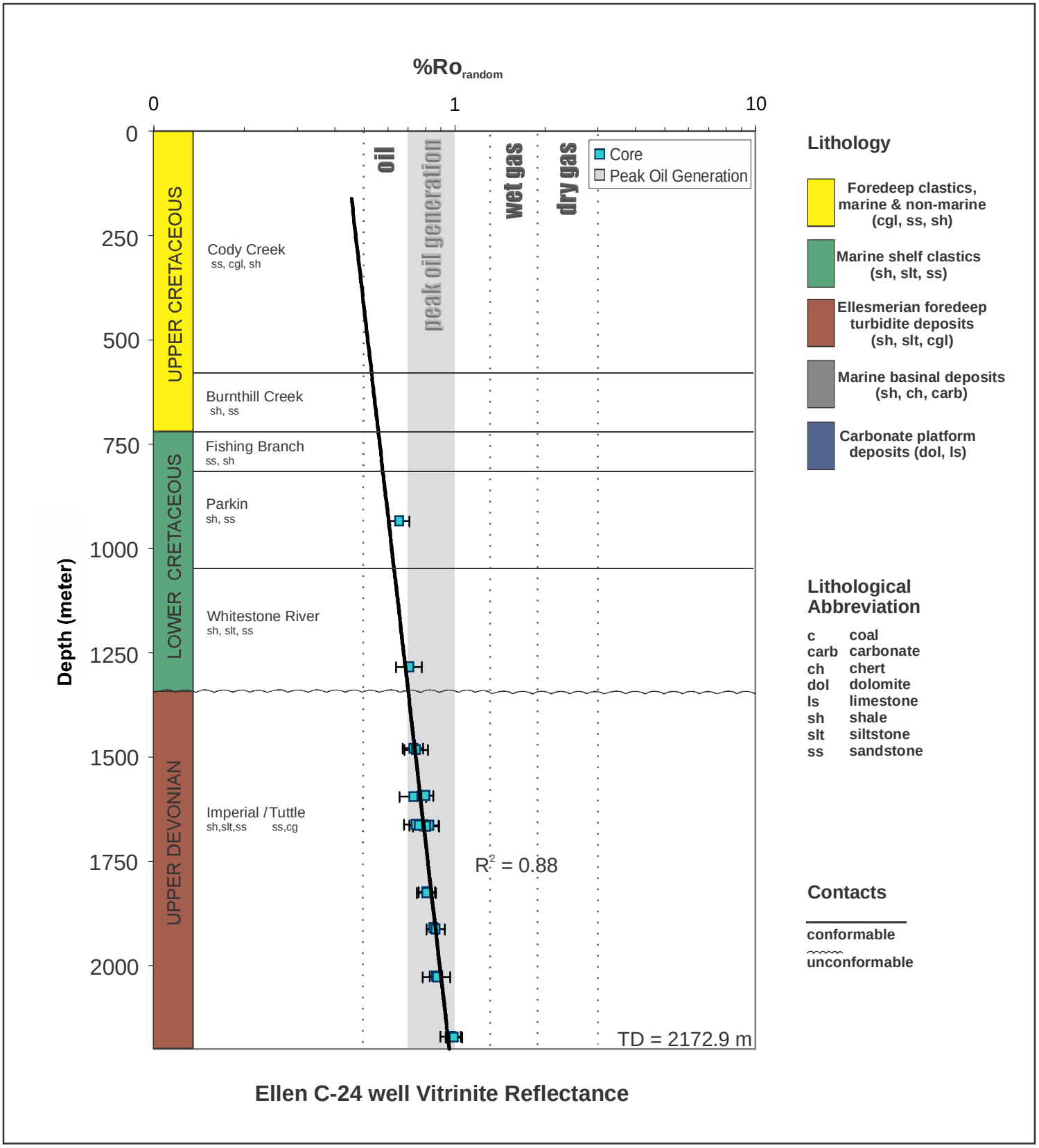

Figure 7. Random vitrinite reflectance values plotted against depth for 18 core samples from the Ellen C-24 well. Formation tops based on Dixon, 1992.

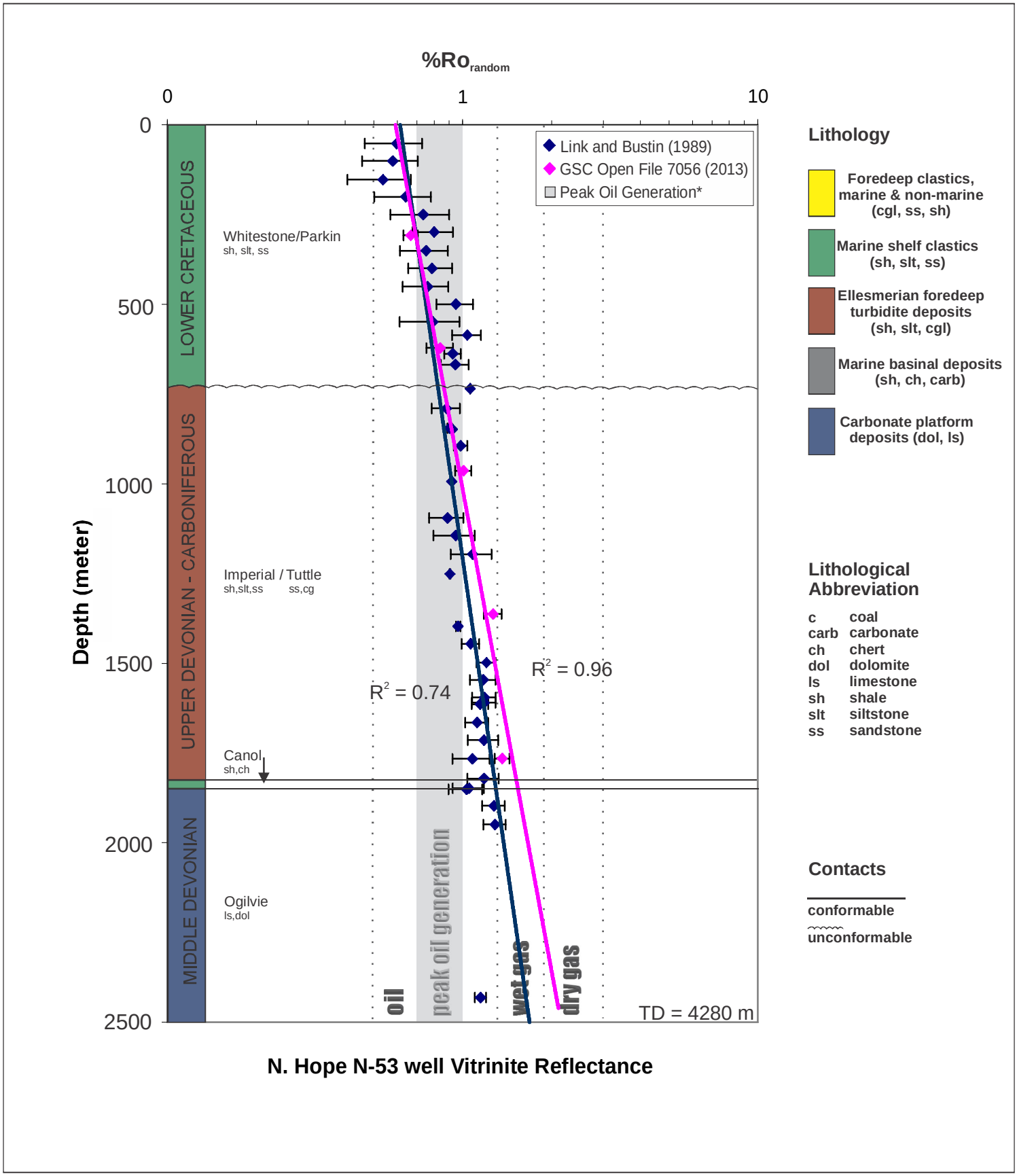

Figure 8: Random vitrinite reflectance (%Ro$_{random}$) values plotted against depth for the N. Hope N-53 well. Five cuttings samples from the GSC (pink) are compared to 40 cuttings samples from the Link and Bustin, 1989 study (blue). Formation tops based on Fraser & Hogue, 2007 and Morrow, 1999.

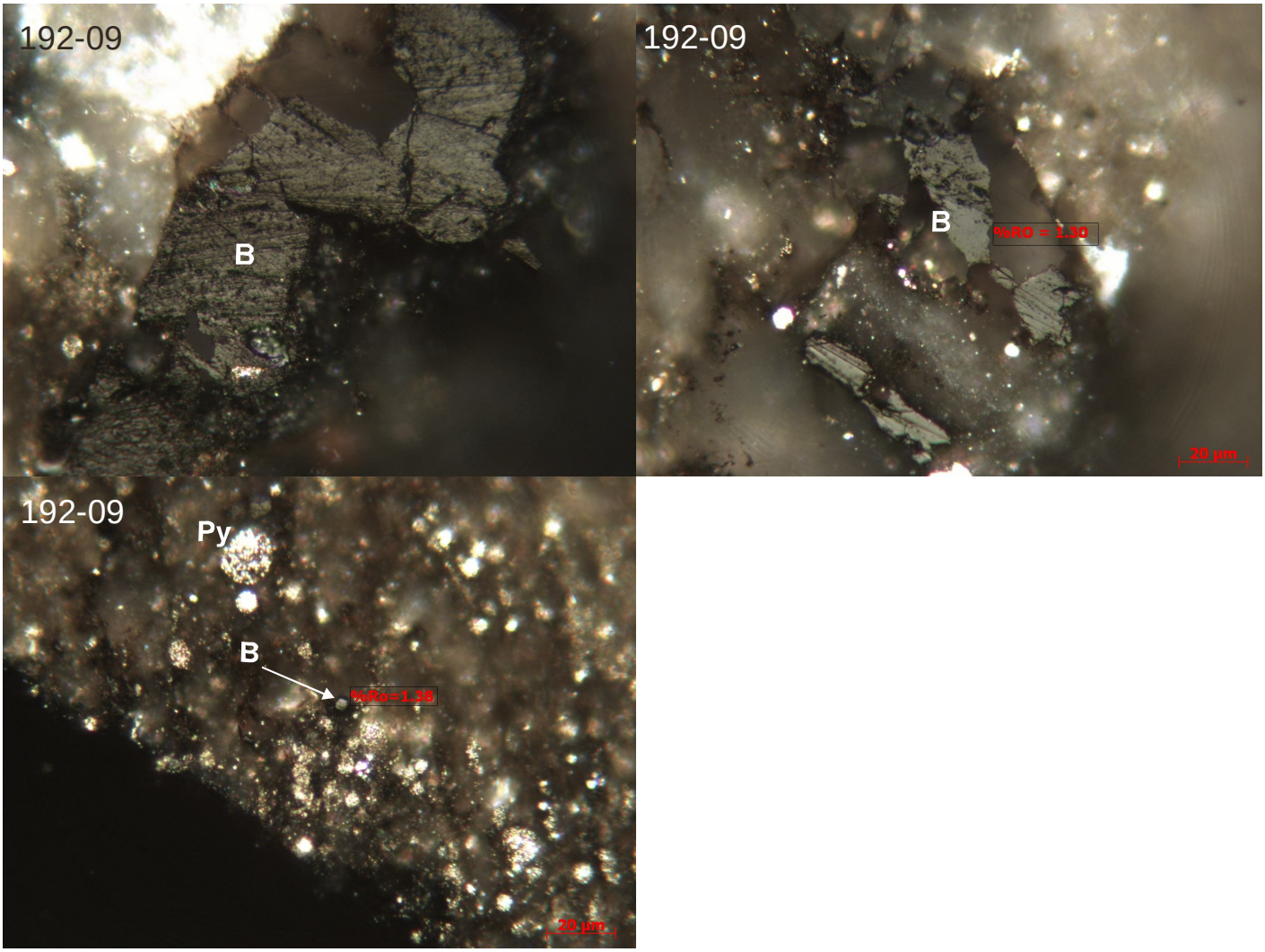

Figure 9. Observed dispersed organic matter in Imperial Formation (1362.8m) from N Hope N-53 well. They consist mainly of interconnected networks of dark amorphous kerogen with minor amounts of non-fluorescing isotropic solid bitumen (B) (%Ro = 1.30) macerals observed between intergranular micropores and microfractures in framboidal pyrite (Py) rich silty shale to fine-grained sandstone matrix. Oil immersion, reflected and UV light microscopy.

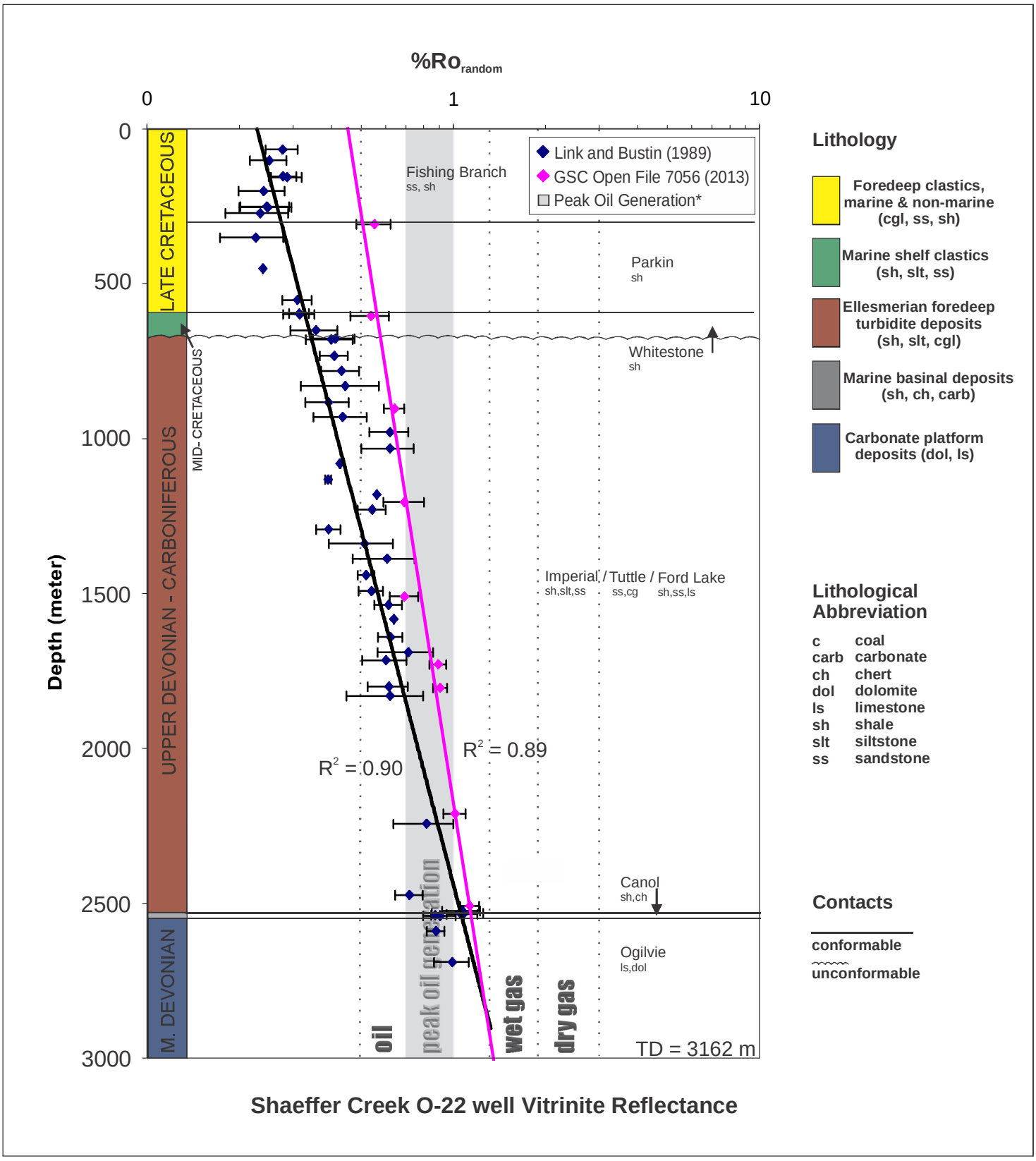

Figure 10: Random vitrinite reflectance (%Ro_{random}) values plotted against depth for the Shaeffer Creek O-22 well. Nine cuttings samples from the GSC (pink) are compared to 48 cuttings samples from the Link and Bustin (1989) study (blue). Formation tops based on Dixon, 1992 and Fraser & Hogue, 2007.

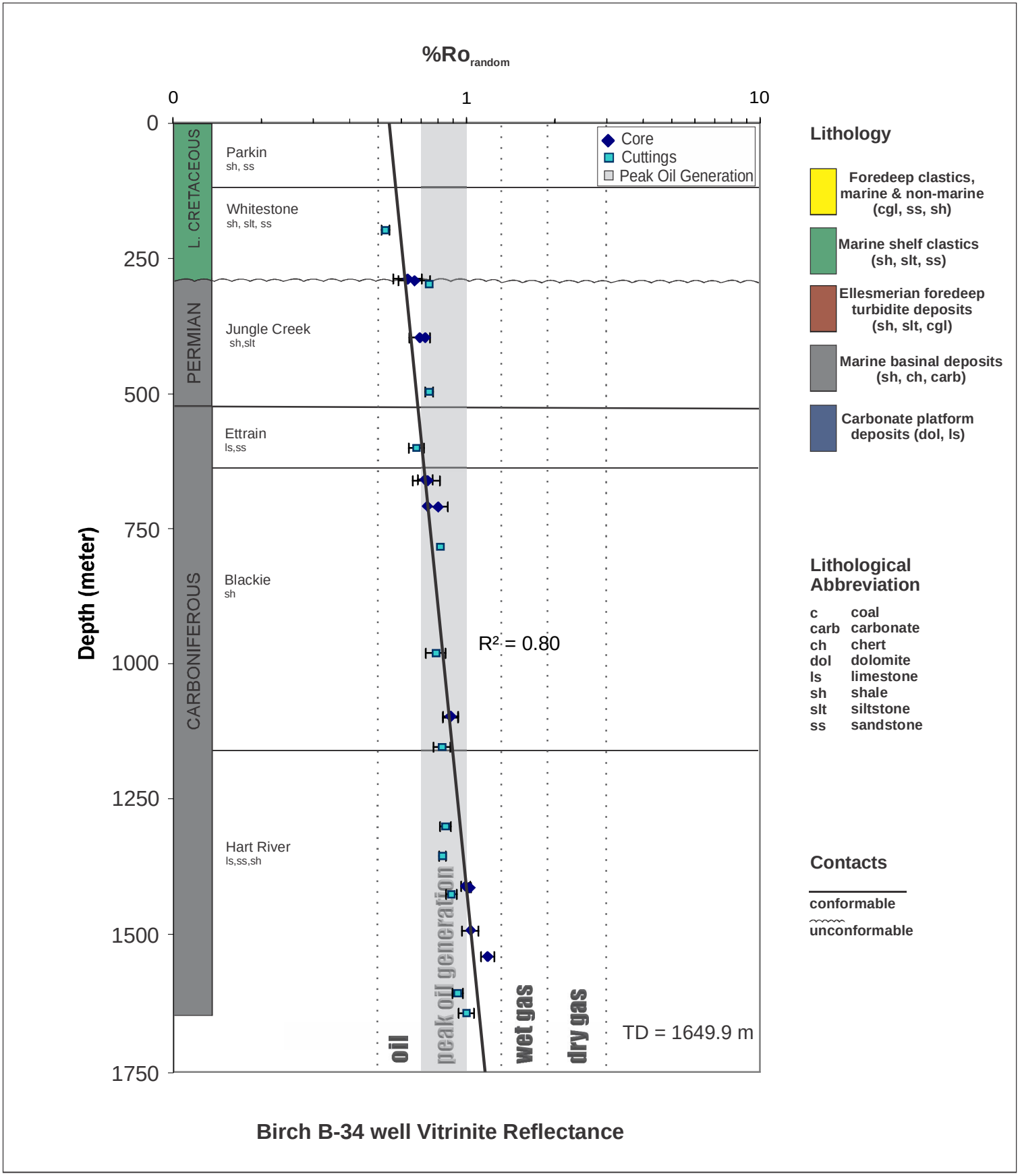

Figure 11. Random vitrinite reflectance values plotted against depth for 14 core and 12 cuttings samples from the Birch B-34 well. Formation tops based on Fraser & Hogue, 2007.

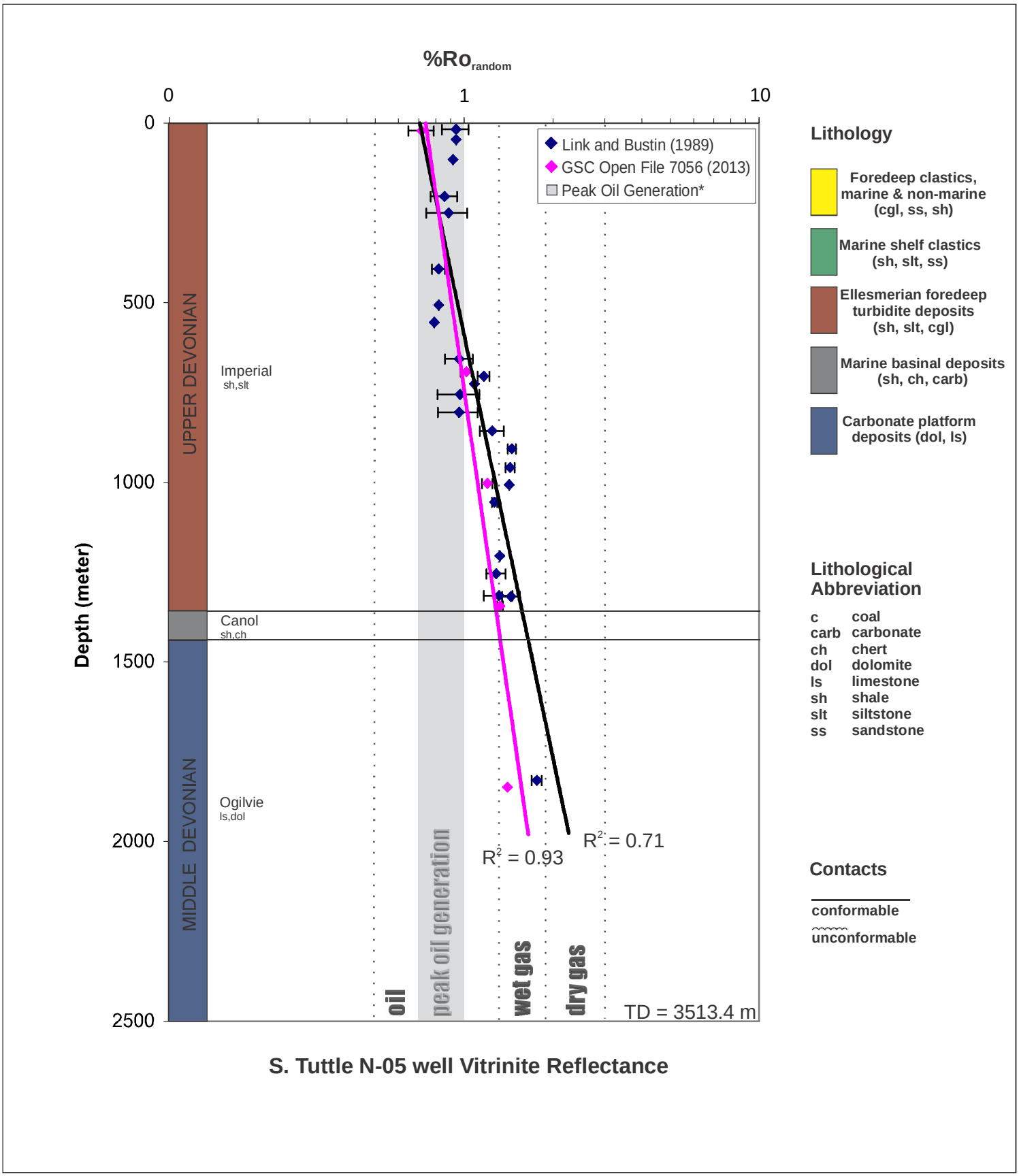

Figure 12: Random vitrinite reflectance (%Ro_{random}) values plotted against depth for the S. Tuttle N-05 well. Two core and three cuttings samples from the GSC (pink) are compared to 23 cuttings samples from the Link and Bustin (1989) study (blue). Formation tops based on Morrow, 1999.

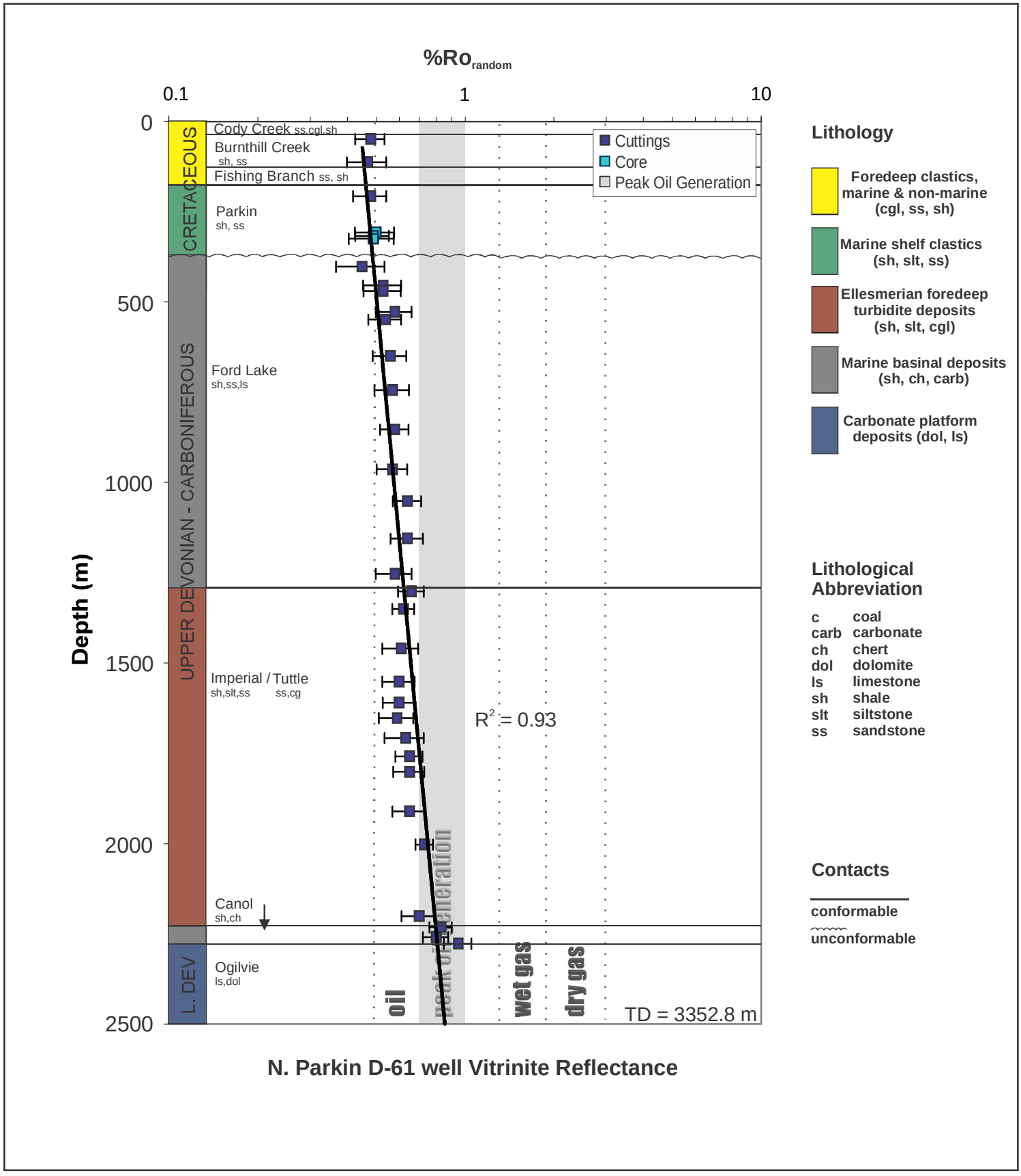

Figure 13. Random vitrinite reflectance values plotted against depth for 3 core and 30 cuttings samples from the North Parkin D-61 well. Formation tops are modified from Dixon, 1992; Pugh, 1983 and Morrow, 1999, based on Lane et al., 2012.

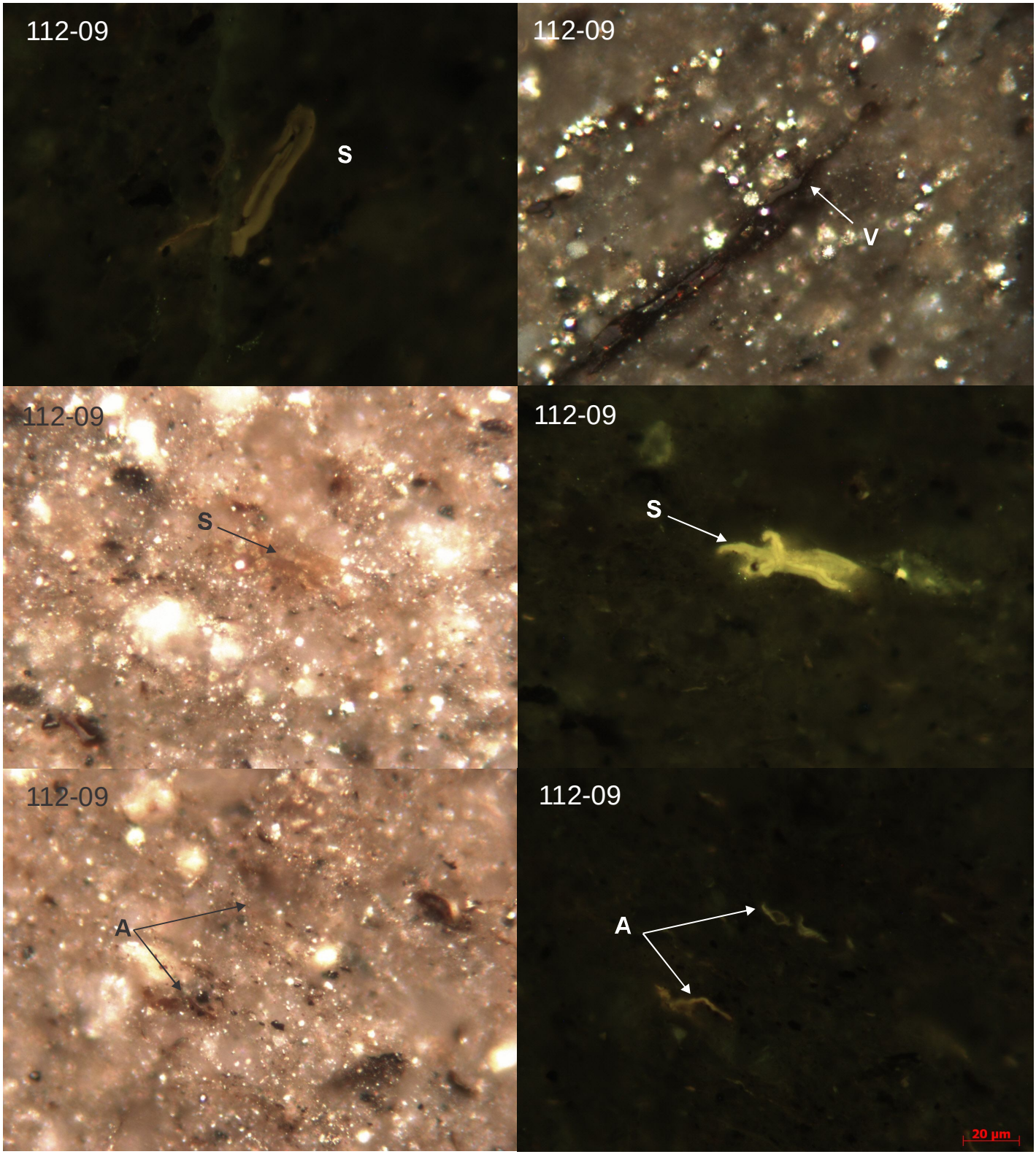

Figure 14. Observed dispersed organic matter in Parkin Formation (324.6m) from N. Parkin D-61 well in the form of mainly dark small lenses of amorphous kerogen with minor amounts of indigenous yellow fluorescing sporinite (S),vitrinite (V), and greenish-yellow alginite (A) macerals in framboidal pyrite rich silty shale marl matrix. Oil immersion, reflected and UV light microscopy.

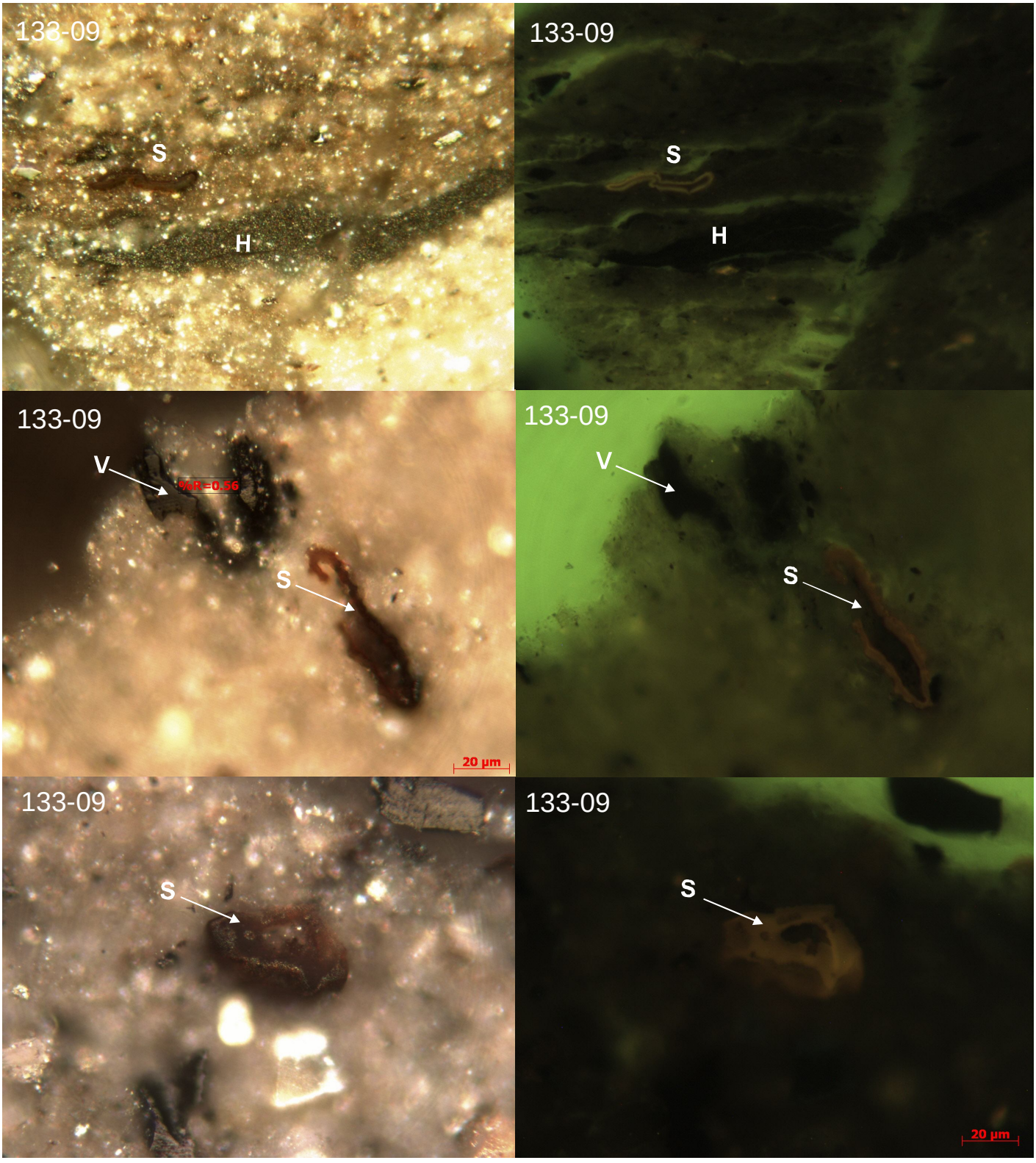

Figure 15: Observed dispersed organic matter in the Imperial Formation (1609.3 m) from N. Parkin D-61 well in the form of mainly small lenses of amorphous kerogen, vitrinite (V), orange fluorescing sporinite (S) semi-concentrated granular hebamorphinite (H) macerals in a pyrite-rich silty shale marl matrix. Oil immersion, reflected and UV light microscopy.

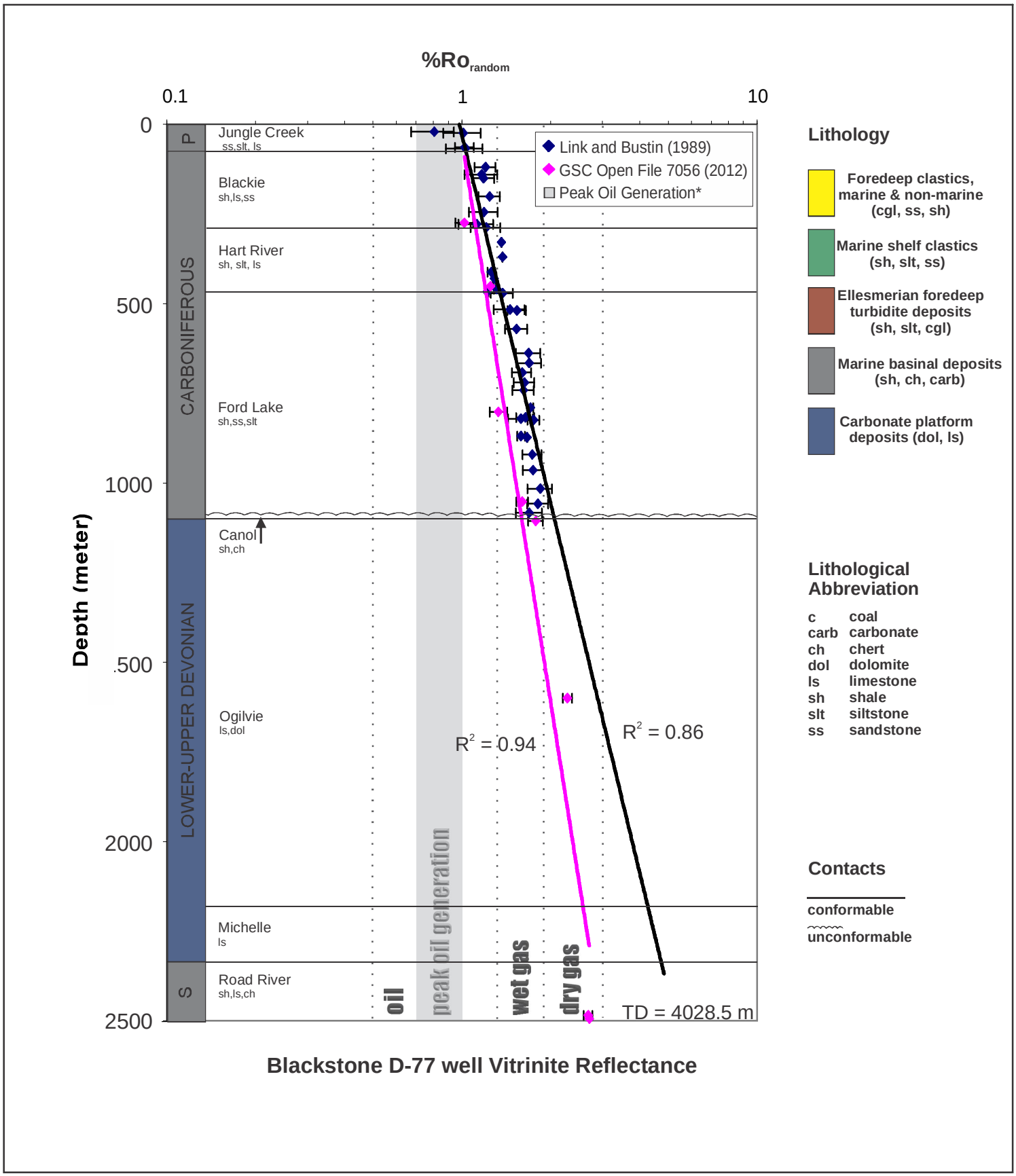

Figure 16: Random vitrinite reflectance ($\%Ro_{random}$) values plotted against depth for the Blackstone D-77 well. Three core and 5 cuttings samples from the GSC (pink) are compared to 37 cuttings samples from the Link and Bustin (1989) study (blue). Formation tops based on Pugh, 1983 and Morrow, 1999.

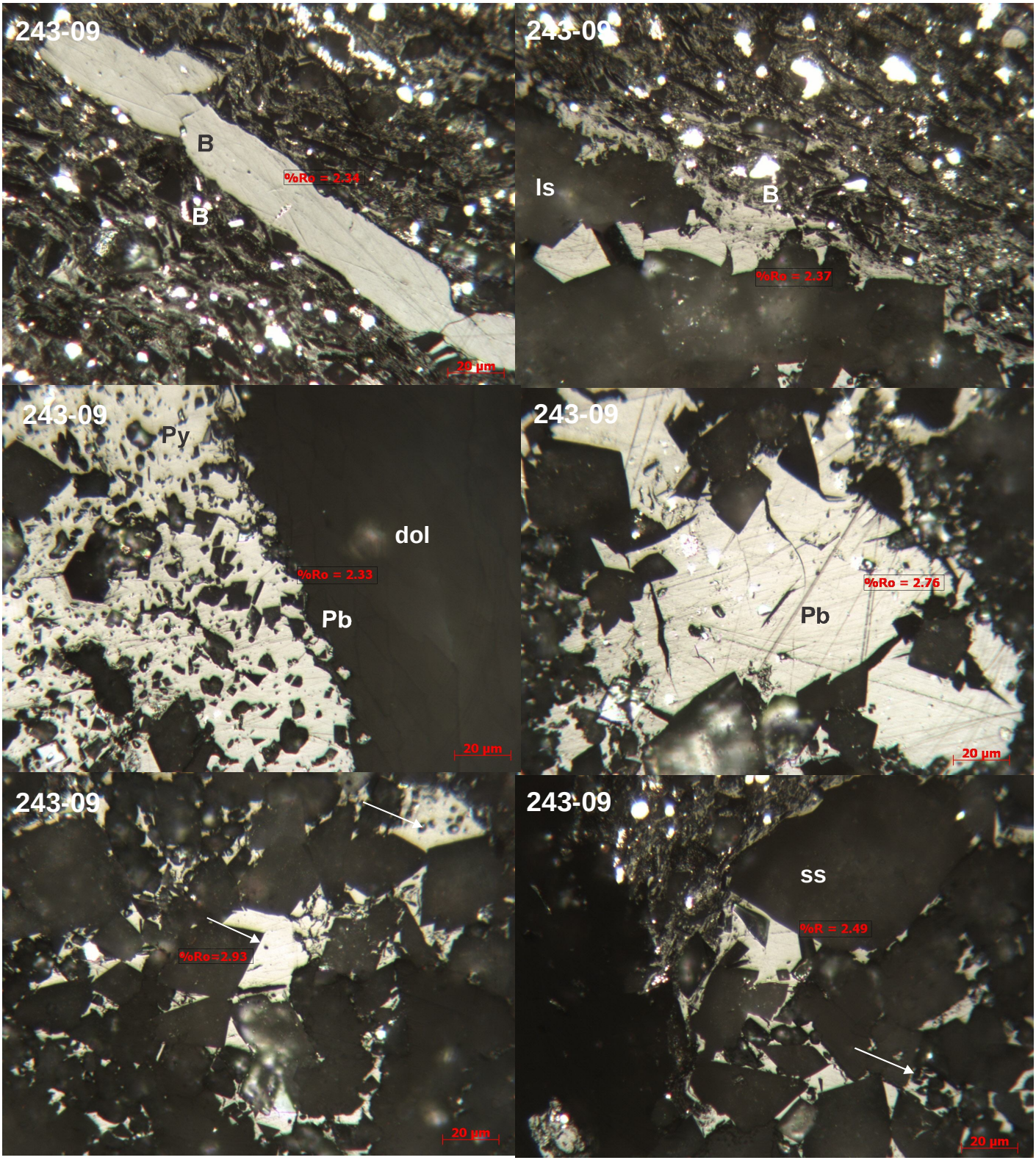

Figure 17. Observed dispersed organic matter in Ogilvie Formation (1600 m) from Blackstone D-77 well. There is a notably high concentration of isotropic solid bitumen (B) and migrated pyrobitumen (Pb) (%Ro = >2.30) macerals, some showing devolatilization vacuoles (arrow) possibly due to thermal cracking, observed between intergranular pores and microfractures in framboidal pyrite (Py) rich angular sandstone grains (ss) to limestone (ls) and dolomite (dol) matrix. Oil immersion, reflected and UV light microscopy.

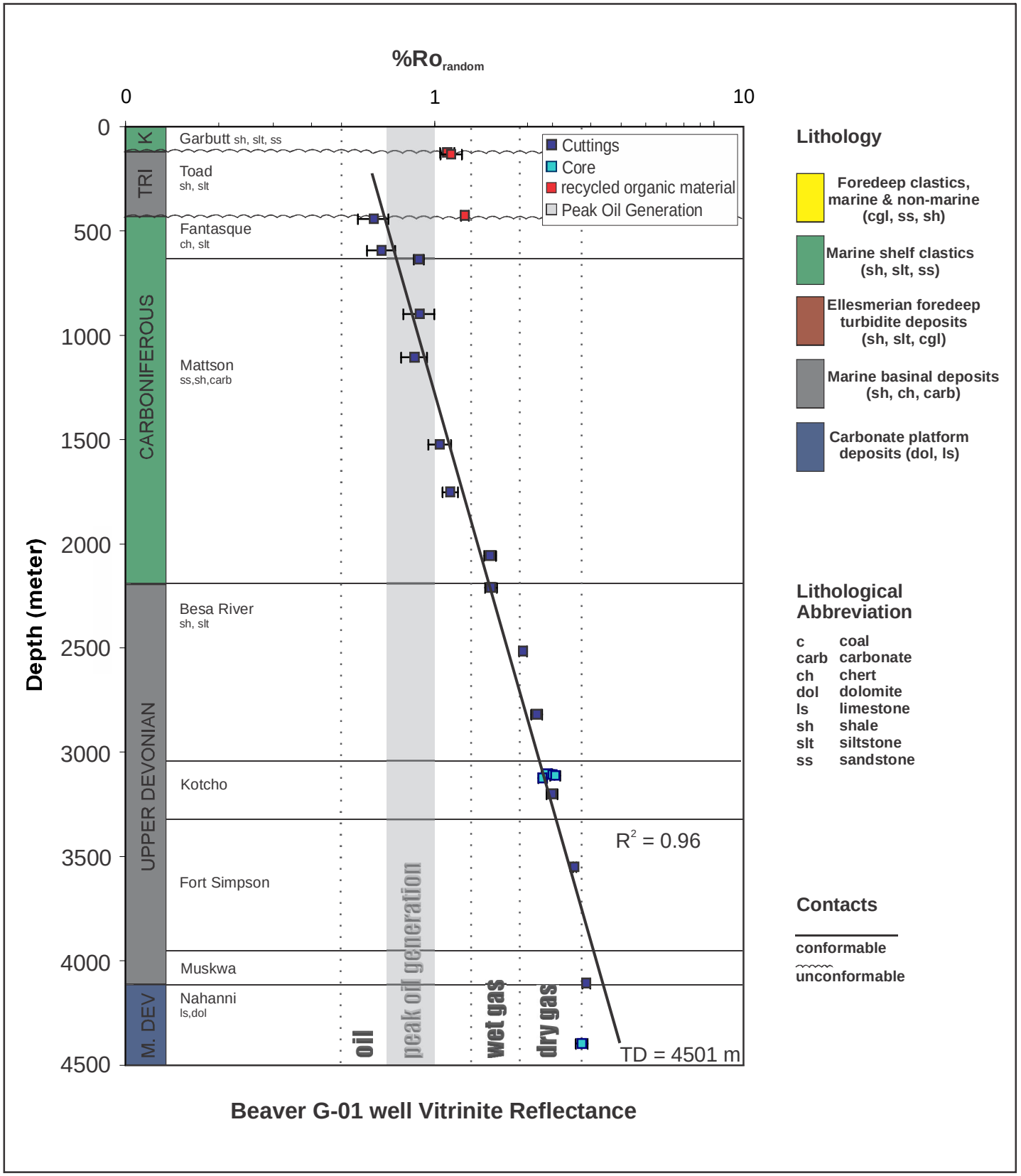

Figure 18: Random vitrinite reflectance (%Ro_{random}) values plotted against depth for 5 core (light blue) and 17 cuttings (navy) samples from the Beaver G-01 well. Formation tops based on Fraser & Hogue, 2007

Table 1. Reflectance data for Ellen C-24 well

GSC (2012)							
Formation	**Depth (m)**	**%Ro_{rand}**	**SD**	**N**	**Pellet #**	**OM Type**	**Sample Type**
Parkin	934.7	0.65	0.05	43	334/09	2	core
Whitestone River	1284.4	0.71	0.07	46	335/09	2	core
Imperial/Tuttle	1479.5	0.73	0.06	26	336/09	2	core
	1482.5	0.75	0.07	28	337/09	2	core
	1592.7	0.80	0.05	27	338/09	2	core
	1595.5	0.73	0.07	41	339/09	2	core
	1661.6	0.74	0.07	40	340/09	2	core
	1663.9	0.83	0.06	23	341/09	2	core
	1664.5	0.76	0.05	11	342/09	3	core
	1666.3	0.81	0.08	16	343/09	3	core
	1823.8	0.81	0.05	29	344/09	2	core
	1826.4	0.81	0.06	26	345/09	2	core
	1909.7	0.85	0.02	4	346/09	2	core
	1912.8	0.87	0.06	28	347/09	2	core
	2025.9	0.87	0.04	28	348/09	2	core
	2028.4	0.88	0.09	33	349/09	2	core
	2170.2	0.97	0.08	35	350/09	2	core
	2172.6	0.99	0.06	31	351/09	2	core

*Organic Matter Type:
2 - vitrinite
3 - Bitumen: vitrinite equivalent = 0.618 x %Ro(bitumen) + 0.40 values (Jacob, 1989)
21- Pyrobitumen: vitrinite equivalent = 0.618 x %Ro(pyrobitumen) +0.40 values (Jacob, 1989)

Table 2. Reflectance data for Western Minerals N. Hope N-53 well

Link & Bustin (1987)									
Formation	**Depth (m)**	**%Ro$_{rand}$**	**SD**	**N**	**Formation**	**Depth (m)**	**%Ro$_{rand}$**	**SD**	**N**
Parkin and Whitestone River	52	0.60	0.13	23	Imperial / Tuttle	1397	0.97	0.02	3
	101	0.58	0.12	13		1446	1.07	0.07	51
	153	0.54	0.13	12		1498	1.20	0.09	10
	201	0.64	0.14	9		1546	1.17	0.12	6
	250	0.74	0.17	8		1595	1.19	0.11	22
	299	0.80	0.13	13		1610	1.18	0.11	12
	351	0.75	0.14	11		1614	1.15	0.07	6
	400	0.79	0.13	14		1665	1.12	0.10	4
	451	0.76	0.13	9		1714	1.18	0.14	5
	500	0.95	0.14	7		1766	1.08	0.16	2
	549	0.79	0.18	9		1821	1.18	0.14	18
	586	1.04	0.12	10	Canol	1848	1.05	0.13	20
	638	0.93	0.06	8	Ogilvie	1851	1.03	0.14	18
	668	0.95	0.10	5		1897	1.28	0.11	9
Imperial / Tuttle	735	1.06	0.00	1		1949	1.29	0.11	14
	790	0.88	0.10	2		2431	1.15	0.05	17
	845	0.90	0.02	2					
	848	0.92	0.00	1					
	894	0.99	0.05	3					
	994	0.92	0.00	1					
	1095	0.89	0.12	8					
	1144	0.95	0.15	4					
	1196	1.08	0.17	17					
	1251	0.91	0.00	2					

GSC (2012)							
Formation	**Depth (m)**	**%Ro$_{rand}$**	**SD**	**N**	**Pellet #**	**OM Type**	**Sample Type**
Whitestone River	307.9	0.67	0.04	11	189/09	2	cuttings
	622	0.84	0.09	7	190/09	2	cuttings
Imperial/ Tuttle	963.4	1.01	0.06	11	191/09	2	cuttings
	1362.8	1.27	0.09	13	192/09	2	cuttings
	1765.2	1.36	0.08	16	193/09	2	cuttings

*Organic Matter Type:
2 - vitrinite
3 - Bitumen: vitrinite equivalent = 0.618 x %Ro(bitumen) + 0.40 values (Jacob, 1989)
21- Pyrobitumen: vitrinite equivalent = 0.618 x %Ro(pyrobitumen) +0.40 values (Jacob, 1989)

Table 3: Vitrinite reflectance data for Shaeffer Creek O-22 well

Link & Bustin (1987)									
Formation	**Depth (m)**	**%Ro$_{rand}$**	**SD**	**N**	**Formation**	**Depth (m)**	**%Ro$_{rand}$**	**SD**	**N**
Fishing Branch	67	0.28	0.033	51	Imperial/ Tuttle	1229	0.54	0.057	2
	101	0.25	0.034	54		1293	0.39	0.036	3
	153	0.28	0.029	52		1339	0.51	0.121	8
	156	0.29	0.033	52		1388	0.61	0.139	4
	201	0.24	0.041	51		1440	0.52	0.032	2
Parkin	250	0.25	0.045	51		1492	0.54	0.049	3
	253	0.25	0.048	20		1537	0.62	0.064	3
	272	0.23	0.054	27		1583	0.64	0.000	1
	351	0.23	0.053	18		1641	0.62	0.057	8
	451	0.24	0.000	1		1690	0.71	0.147	5
	552	0.31	0.034	4		1715	0.60	0.100	11
Whitestone River	595	0.31	0.023	3		1800	0.62	0.092	5
	598	0.32	0.037	2		1830	0.62	0.174	3
	650	0.36	0.062	9		2243	0.82	0.181	5
	677	0.41	0.064	14		2474	0.72	0.074	3
Imperial/ Tuttle	680	0.40	0.069	15		2525	1.07	0.151	4
	732	0.41	0.042	4		2532	1.05	0.200	17
	781	0.43	0.061	7	Canol	2535	1.08	0.123	4
	830	0.44	0.126	7	Ogilvie	2538	0.87	0.029	6
	882	0.39	0.063	8		2541	0.91	0.109	36
	930	0.44	0.086	5		2590	0.88	0.058	27
	979	0.62	0.090	6		2690	0.99	0.129	12
	1031	0.62	0.120	3					
	1080	0.43	0.002	3					
	1132	0.39	0.009	2					
	1180	0.56	0.000	1					

GSC (2012)							
Formation	**Depth (m)**	**%Ro$_{rand}$**	**SD**	**N**	**Pellet #**	**OM Type***	**Sample Type**
Parkin	308	0.55	0.071	54	67/09	2	cuttings
Whitestone River	604	0.54	0.078	31	68/09	2	cuttings
Imperial/ Tuttle	902	0.64	0.049	17	69/09	2	cuttings
	1204	0.69	0.033	15	70/09	2	cuttings
	1509	0.69	0.074	27	71/09	2	cuttings
	1729	0.89	0.056	52	77/09	2	cuttings
	1805	0.91	0.048	24	72/09	2	cuttings
	2210	1.01	0.085	34	73/09	2	cuttings
	2509	1.13	0.08	31	74/09	2	cuttings

*Organic Matter Type:

2 - vitrinite

3 - Bitumen: vitrinite equivalent = 0.618 x %Ro(bitumen) + 0.40 value s (Jacob, 1989)

21- Pyrobitumen: vitrinite equivalent = 0.618 x %Ro(pyrobitumen) +0.40 value s (Jacob, 1989)

Table 4. Reflectance data for Birch B-34 well

GSC (2013)							
Formation	**Depth (m)**	**%Ro$_{rand}$**	**SD**	**N**	**Pellet #**	**OM Type***	**Sample Type**
Whitestone River	198	0.61	0.04	7	246/13	2	cuttings
	288	0.64	0.07	25	133/10	2	core
Jungle Creek	291	0.67	0.08	22	134/10	2	core
	299	0.75		1	247/13	2	cuttings
	396	0.73		1	135/10	2	core
	398	0.70	0.06	14	136/10	2	core
	497	0.75	0.02	2	248/13	2	cuttings
Ettrain	601	0.68	0.04	4	249/13	2	cuttings
Blackie	659	0.73	0.04	21	137/10	2	core
	661	0.74	0.08	15	138/10	2	core
	708	0.74		1	139/10	2	core
	710	0.81	0.06	5	140/10	2	core
	784	0.82		1	250/13	2	cuttings
	979	0.79	0.06	6	251/13	2	cuttings
	1096	0.89	0.05	20	141/10	2	core
	1099	0.89	0.05		142/10	2	core
	1152	0.83	0.05	7	252/13	2	cuttings
Hart River	1299	0.85	0.04	11	253/13	3	cuttings
	1354	0.83	0.02	4	254/13	3	cuttings
	1409	1.00	0.04		143/10	3	core
	1412	1.03	0.01	2	144/10	2	core
	1424	0.89	0.04	7	255/13	3	cuttings
	1492	1.04	0.07	27	145/10	3	core
	1539	1.19	0.06	9	146/10	3	core
	1607	0.94	0.04	5	256/13	2	cuttings
	1643	1.01	0.06	13	257/13	2	cuttings

*Organic Matter Type:
2 - vitrinite
3 - Bitumen: vitrinite equivalent = 0.618 x %Ro(bitumen) + 0.40 values (Jacob, 1989)
21- Pyrobitumen: vitrinite equivalent = 0.618 x %Ro(pyrobitumen) +0.40 values (Jacob, 1989)

Table 5. Reflectance data for Socony Mobil WM S. Tuttle N-05 well

Link & Bustin (1987)				
Formation	**Depth (m)**	**%Ro$_{rand}$**	**SD**	**N**
Imperial	18	0.94	0.098	6
	46	0.94	0.000	1
	101	0.92	0.000	1
	204	0.86	0.087	3
	250	0.88	0.141	9
	406	0.82	0.042	6
	506	0.82	0.000	1
	555	0.79	0.000	1
	656	0.96	0.103	5
	705	1.17	0.055	6
	726	1.08	0.000	1
	756	0.97	0.156	7
	805	0.96	0.149	5
	857	1.25	0.117	10
	906	1.45	0.046	6
	958	1.43	0.048	5
	1007	1.42	0.000	1
	1055	1.27	0.027	3
	1205	1.32	0.000	1
	1254	1.29	0.096	15
	1315	1.31	0.147	5
	1318	1.44	0.100	12
Ogilvie	1830	1.76	0.073	7

GSC (2013)							
Formation	**Depth (m)**	**%Ro$_{rand}$**	**SD**	**N**	**Pellet #**	**OM Type**	**Sample Type**
Imperial	21	0.72	0.07	31	05/09	2	core
	692	1.02	0.04	11	06/09	2	core
	1003	1.20	0.05	16	07/09	2	cuttings
	1345	1.32	0.03	4	03/09	2	cuttings
Ogilvie	1849	1.40		1	04/09	2	cuttings

*Organic Matter Type:
2 - vitrinite
3 - Bitumen: vitrinite equivalent = 0.618 x %Ro(bitumen) + 0.40 values (Jacob, 1989)
21- Pyrobitumen: vitrinite equivalent = 0.618 x %Ro(pyrobitumen) +0.40 values (Jacob, 1989)

Table 6. Reflectance data for N. Parkin D-61 well

GSC (2012)							
Formation	**Depth (m)**	**%Ro_{rand}**	**SD**	**N**	**Pellet #**	**OM Type**	**Sample Type**
Burnthill Creek	50.3	0.48	0.054	27	114/09	2	cuttings
	112.8	0.47	0.072	47	115/09	2	cuttings
Parkin	207.3	0.48	0.062	46	116/09	2	cuttings
	307.1	0.50	0.075	12	110/09	2	core
	317.0	0.49	0.063	20	111/09	2	core
	324.6	0.49	0.085	47	112/09	2	core
Ford Lake	402.3	0.45	0.084	11	117/09	2	cuttings
	454.2	0.53	0.078	20	118/09	2	cuttings
	469.4	0.53	0.077	25	119/09	2	cuttings
	527.3	0.58	0.081	43	120/09	2	cuttings
	548.6	0.54	0.069	38	121/09	2	cuttings
	649.2	0.56	0.072	37	122/09	2	cuttings
	743.7	0.57	0.076	43	123/09	2	cuttings
	853.4	0.58	0.063	47	124/09	2	cuttings
	963.2	0.57	0.068	44	125/09	2	cuttings
	1051.6	0.64	0.070	25	126/09	2	cuttings
	1155.2	0.64	0.080	11	127/09	2	cuttings
	1252.7	0.58	0.081	36	128/09	2	cuttings
Imperial/ Tuttle	1301.5	0.66	0.066	42	129/09	2	cuttings
	1350.3	0.62	0.05	49	130/09	2	cuttings
	1460.0	0.61	0.084	41	131/09	2	cuttings
	1551.4	0.60	0.08	43	132/09	2	cuttings
	1609.3	0.60	0.073	38	133/09	2	cuttings
	1652.0	0.59	0.079	36	134/09	2	cuttings
	1706.9	0.63	0.095	37	135/09	2	cuttings
	1758.7	0.65	0.069	30	136/09	2	cuttings
	1801.4	0.65	0.077	29	137/09	2	cuttings
	1911.1	0.65	0.081	20	138/09	2	cuttings
	2002.5	0.73	0.050	19	139/09	2	cuttings
	2200.7	0.70	0.090	21	140/09	2	cuttings
Canol	2231.1	0.83	0.073	19	141/09	2	cuttings
	2258.6	0.80	0.079	25	142/09	2	cuttings
	2276.9	0.95	0.10	15	143/09	2	cuttings

*Organic Matter Type:
2 - vitrinite
3 - Bitumen: vitrinite equivalent = 0.618 x %Ro(bitumen) + 0.40 values (Jacob, 1989)
21- Pyrobitumen: vitrinite equivalent = 0.618 x %Ro(pyrobitumen) +0.40 values (Jacob, 1989)

Table 7: Vitrinite reflectance data for Blackstone D-77 well

Link & Bustin (1987)				
Formation	**Depth (m)**	**%Ro$_{rand}$**	**SD**	**N**
Jungle Creek	21	0.805	0.133	25
	24	1.011	0.146	25
	64	1.021	0.075	14
Blackie	67	1.028	0.146	10
	119	1.201	0.097	24
	140	1.168	0.148	39
	150	1.183	0.103	19
	201	1.240	0.103	18
	244	1.188	0.132	8
	278	1.123	0.151	13
	287	1.208	0.139	2
Hart River	329	1.362	0.000	1
	369	1.372	0.000	1
	412	1.257	0.037	2
	430	1.287	0.017	2
	458	1.311	0.027	2
	467	1.218	0.012	2
Ford Lake	470	1.371	0.117	20
	516	1.455	0.172	9
	519	1.536	0.110	10
	570	1.532	0.131	34
	638	1.682	0.162	7
	665	1.691	0.161	7
	692	1.599	0.120	11
	720	1.628	0.128	18
	741	1.617	0.136	24
	790	1.706	0.037	2
	817	1.641	0.115	3
	821	1.584	0.151	6
	824	1.746	0.081	3
	869	1.585	0.047	6
	872	1.660	0.000	1
	921	1.732	0.129	4
	964	1.745	0.138	3
	1016	1.843	0.177	5
	1058	1.812	0.150	6
	1083	1.692	0.171	12

GSC (2012)							
Formation	**Depth (m)**	**%Ro$_{rand}$**	**SD**	**N**	**Pellet #**	**OM Type**	**Sample Type**
Blackie	274	1.02	0.07	9	246/09	2	cuttings
Hart River	451	1.25	0.05	10	247/09	2	cuttings
Ford Lake	802	1.33	0.09	10	248/09	2	cuttings
	1052	1.60	0.07	17	249/09	3	cuttings
Ogilvie	1107	1.78	0.101	18	250/09	2	cuttings
	1600	2.28	0.08	45	243/09	3	core
Road River Gp	2484	2.68	0.09	11	244/09	2	core
	2494	2.7		16	245/09	2	core

*Organic Matter Type:

2 - vitrinite

3 - Bitumen: vitrinite equivalent = 0.618 x %Ro(bitumen) + 0.40 values (Jacob, 1989)

21- Pyrobitumen: vitrinite equivalent = 0.618 x %Ro(pyrobitumen) +0.40 values (Jacob, 1989)

Table 8. Reflectance data for Beaver G-01 well

GSC (2012)							
Formation	**Depth (m)**	**%Ro_{rand}**	**SD**	**N**	**Pellet #**	**OM Type**	**Sample Type**
Toad	125	1.10	0.06	13	116/10	2	cuttings
	134	1.14	0.09	5	117/10	2	cuttings
	427	1.25	0.04	10	118/10	2	cuttings
Fantasque	442	0.64	0.07	27	119/10	2	cuttings
	594	0.67	0.07	12	120/10	2	cuttings
Mattson	637	0.89	0.03	3	121/10	2	cuttings
	899	0.90	0.10	4	122/10	2	cuttings
	1106	0.86	0.08	11	123/10	2	cuttings
	1524	1.04	0.09	14	124/10	2	cuttings
	1753	1.13	0.06	15	125/10	2	cuttings
	2057	1.51	0.07	14	126/10	2	cuttings
Besa River	2210	1.52	0.07	4	127/10	2	cuttings
	2515	1.93	0.06	17	128/10	2	cuttings
	2819	2.14	0.09	21	129/10	2	cuttings
Kotcho	3102	2.31	0.10	29	352/09	2	core
	3107	2.41	0.03	9	353/09	2	core
	3113	2.46	0.09	14	354/09	2	core
	3124	2.24	0.07	11	355/09	2	core
	3200	2.40	0.11	28	130/10	2	cuttings
Ft Simpson	3551	2.84	0.10	10	131/10	2	cuttings
Muskwa	4109	3.10	0.11	16	132/10	3	cuttings
Nahanni	4396	3.00	0.13	39	356/09	21	core

*Organic Matter Type:

2 - vitrinite

3 - Bitumen: vitrinite equivalent = 0.618 x %Ro(bitumen) + 0.40 values (Jacob, 1989)

21- Pyrobitumen: vitrinite equivalent = 0.618 x %Ro(pyrobitumen) +0.40 values (Jacob, 1989)